

Review

# Performance Assessment of Cellulose Paper Impregnated in Nanofluid for Power Transformer Insulation Application: A Review

Andrew Adewunmi Adekunle , Samson Okikiola Oparanti and Issouf Fofana \* 

Research Chair on the Aging of Power Network Infrastructure (ViAHT), University of Quebec at Chicoutimi, Chicoutimi, QC G7H 2B1, Canada

\* Correspondence: ifofana@uqac.ca

**Abstract:** Insulation cellulose paper is a basic measure for a power transformer's remaining useful life, and its advantageous low cost, electrical, and mechanical properties have made it an extensive insulation system when impregnated in a dielectric liquid. Cellulose paper deteriorates as a result of ageing due to some chemical reactions like pyrolysis (heat), hydrolysis (moisture), and oxidation (oxygen) that affects its degree of polymerization. The condition analysis of cellulose paper has been a major concern since the collection of paper samples from an operational power transformer is almost impossible. However, some chemicals generated during cellulose paper deterioration, which were dissolved in dielectric liquid, have been used alternatively for this purpose as they show a direct correlation with the paper's degree of polymerization. Furthermore, online and non-destructive measurement of the degree of polymerization by optical sensors has been proposed recently but is yet to be available in the market and is yet generally acceptable. In mitigating the magnitude of paper deterioration, some ageing assessments have been proposed. Furthermore, researchers have successfully enhanced the insulating performance of oil-impregnated insulation paper by the addition of various types of nanoparticles. This study reviews the ageing assessment of oil-paper composite insulation and the effect of nanoparticles on tensile strength and electrical properties of oil-impregnated paper insulation. It includes not only significant tutorial elements but also some analyses, which open the door for further research on the topic.



**Citation:** Adekunle, A.A.; Oparanti, S.O.; Fofana, I. Performance Assessment of Cellulose Paper Impregnated in Nanofluid for Power Transformer Insulation Application: A Review. *Energies* **2023**, *16*, 2002. <https://doi.org/10.3390/en16042002>

Academic Editor: Gabriela Huminic

Received: 30 January 2023

Revised: 13 February 2023

Accepted: 14 February 2023

Published: 17 February 2023



**Copyright:** © 2023 by the authors. Licensee MDPI, Basel, Switzerland. This article is an open access article distributed under the terms and conditions of the Creative Commons Attribution (CC BY) license (<https://creativecommons.org/licenses/by/4.0/>).

**Keywords:** cellulose paper; nanofluid; ageing; surface charge; electrical properties

## 1. Introduction

Nowadays, a power transformer is the key element in an electrical grid that is needed to meet fast-growing electricity demand [1]. Equipment failure leads to blackouts, loss of energy, and also decreases the reliability of the system, which has a consequential impact on power quality [2,3]. The reliability of power equipment is crucial to our entire society, so statistical analysis has been carried out on transformer accidents and it was revealed that an oil-paper insulation system, among others, has been the main cause of transformer insulation failure [4,5]. Oil-immersed transformers are presently the majority of power transformers used in power systems [6–8]. Life expectancy and safe operation of an oil-immersed power transformer are mainly decided by the mechanical, physicochemical, and electrical properties of its composite insulation system [9–11]. Transformer core windings are exposed to extensive electromagnetic stresses in the course of a power network operation. Therefore, this equipment experiences mechanical and electrical stresses in its entire part, so its power rating is greatly increased to meet the high demand for ever-increasing voltage levels [12]. Liquids and solids are the two materials that majorly constitute the power transformer composite insulation system [13–16]. Therefore, insulation in power transformers has been standardized and accepted to take the form of paper in insulating oil, since it possesses desirable physical, chemical, and electrical properties [17]. During

periodic operations, the degradation of oil-impregnated paper insulation occurs as a result of various stresses such as chemical, mechanical, thermal, and electrical stresses on the materials that influence the life expectancy of the power equipment [18,19].

Solid insulations are majorly cellulose-based and are used in distinct forms such as Kraft paper and pressboard, as they are porous materials that serve as the principal insulators for winding conductors. They function as materials that prevent electric current flow among the conductors and are likewise impregnated in an insulating fluid to increase cellulose life span as well as to enhance the dielectric characteristics that will enable it to act as a medium of cooling [20–22]. Kraft paper, known as the thin insulation, is usually wrapped around the winding conductors of the power transformer to create a gap for the circulation of insulating oil, while pressboards are the thick insulation usually infused between the wrapped conductor layers. Additionally, sizeable pressboard sheets are usually wrapped around the whole winding, which serves as a barrier to prevent viable direct breakdown through the insulating oil [22]. However, more attention and interest is given to Kraft paper by researchers as a result of high thermal stresses on Kraft paper's inner layer around the conductors, which is about 95 °C, while the temperature of the pressboard is considered to be lower than the insulating oil temperature, which ranges from 60 to 80 °C [23]. Papers employed in solid insulation are fabricated from unbleached softwood pulp in either the Kraft or sulphate process. This unbleached Kraft paper contains cellulose, hemicellulose, and lignin, at percentages of 78–80%, 10–20%, and 2–6%, respectively [24,25]. The percentages of cellulose, hemicellulose, and lignin in dry wood Kraft paper are 40–50%, 10–30%, and 20–30%, respectively [26,27]. The cellulose chemical chain that has the highest percentage is formed when the anhydroglucoses are linked together by glycosidic bonds [28,29]. Cellulose chemical structure is given in Figure 1 and the molecular empirical formula is  $(C_6H_{10}O_5)_n$  where the mass fractions are 44.44% carbon, 6.17% hydrogen, 49.39% oxygen, and  $n$  is the degree of polymerization [30].

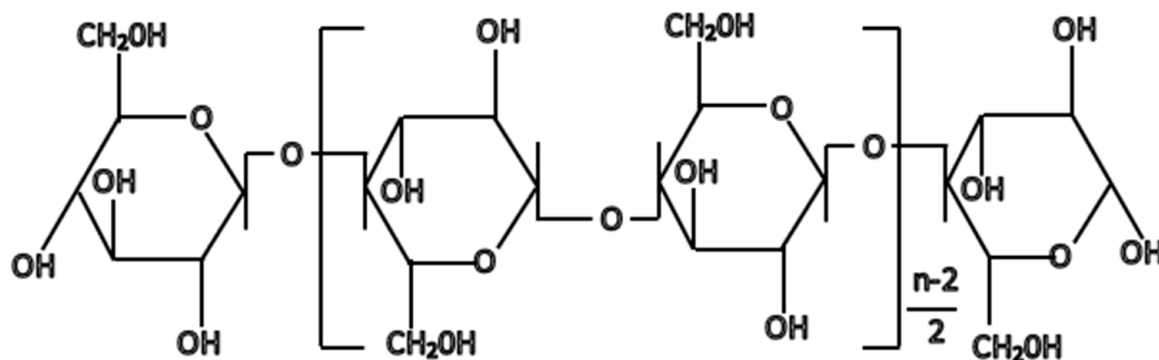


Figure 1. Cellulose molecular chemical structure.

During paper insulation deterioration, breakdown tends to occur in hydrogen bonds, shortening the molecular chain of the cellulose. This leads to the formation of some chemical products such as derivatives of furan, carbondioxide, and carbonmonoxide that later dissolve in the insulating oil [31,32]. Moreover, deterioration mechanisms often occur in the presence of moisture (hydrolysis), oxygen (oxidation), and heat (pyrolysis) [33–35]. Moisture accumulates increasingly as a result of a progressive increase in the hydrolysis rate of the insulation system [36,37]. This accumulated moisture may be a result of moisture penetrating through the oxidation of oil, seals, and cellulose degradation [38]. Oxidation in cellulose paper is a slow reaction process that occurs when the cellulose hydroxyl groups weaken the glycosidic linkage as a result of oxygen attack [39]. Pyrolysis often occurs around the hot spot in the paper as a result of heat in the absence of oxidizing agents and moisture. Figures 2 and 3 show the chemical structures of hydrolysis and pyrolysis mechanisms in cellulose, respectively [40]. Substitution and reclaiming of insulating oil will not increase the life span of cellulose in power transformers, which makes the degra-

gradation of paper made from cellulose a major consideration for a useful and functional transformer's lifetime [41,42]. Fault takes place when there is a decrease in the paper's mechanical strength to the level of being fragile and pre-disposed to damage through mechanical motion [43]. However, the degree of polymerization with time gives correct insight into the paper insulation degradation process [44]. The degree of polymerization value shows the average polymer length of cellulose molecules; as such, a lower degree of polymerization of the sample implies greater degradation [45]. Therefore, mechanical strength (tensile strength), which concerns hydrogen bonding between the oriented linear chain of the cellulose, and the degree of polymerization, which is the average number of glycosidic rings in the macromolecules of cellulose, determine the integrity of paper insulation [23,28,46]. The temperature of the insulating paper environment in the transformer is always greater than the ambient temperature during operation, which causes the paper undergoing thermal ageing to be brittle as well as lose its electrical and mechanical performance. As a result, precise and rigid requirements were placed on paper insulation according to ASTM D149 standards [47]. Presently, cellulose insulating paper has some disadvantages that need attention. Cellulose paper thermal stability governs the transformer lifetime as an increase in temperature changes the cellulose structure. The cellulose insulating paper properties are deteriorated and can even lead to the cellulose paper falling away from the winding. As an effect, the insulating oil impurities increase, thereby affecting the thermal dissipation of conducting materials as well as the overall insulating properties of power transformers [48]. Cellulose paper mechanical strength predicts the lifetime of the transformer as the cellulose structure is also changed and damaged with a decrease in mechanical strength [49]. The cellulose paper dielectric constant is said to increase with a decrease in electric field distribution and vice-versa. Therefore, breakdown occurs in the insulation system due to uneven electric field distribution [50]. Lastly, the cellulose paper's hydrophilic nature will also predict the transformer's lifetime as the transformer's ageing state is determined by the amount of moisture content [51]. This strong hydrophilic nature is a result of extensive polar groups in the cellulose molecules, thereby accelerating paper degradation and increasing conductivity [52]. Therefore, each one percent increase in moisture content doubles the cellulose rate of hydrolytic ageing [53], and for every increase in moisture by 0.5%, the life span of the power transformer is reduced by half [54].

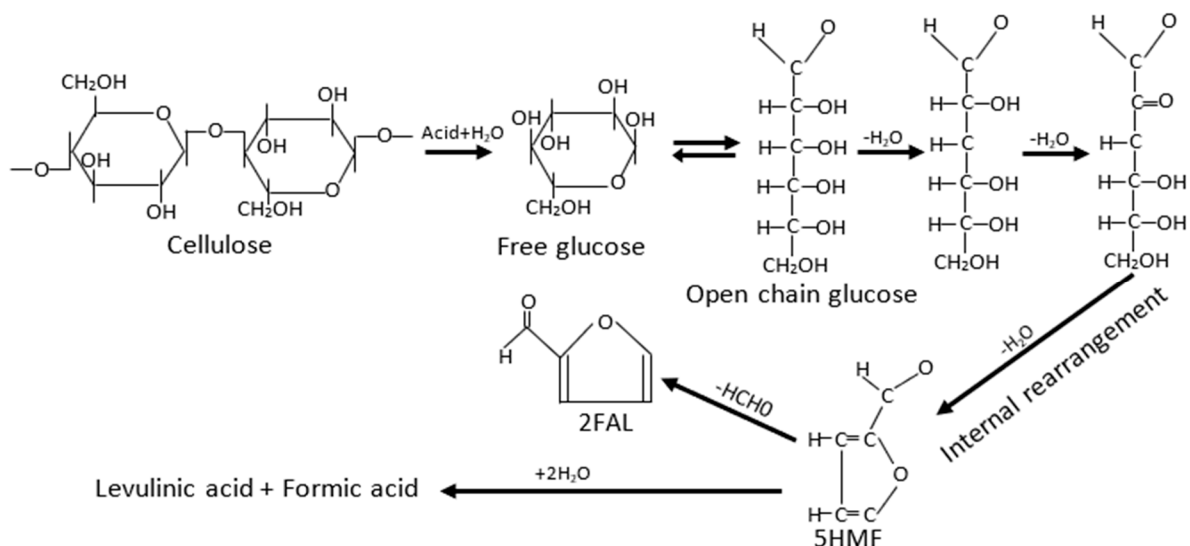
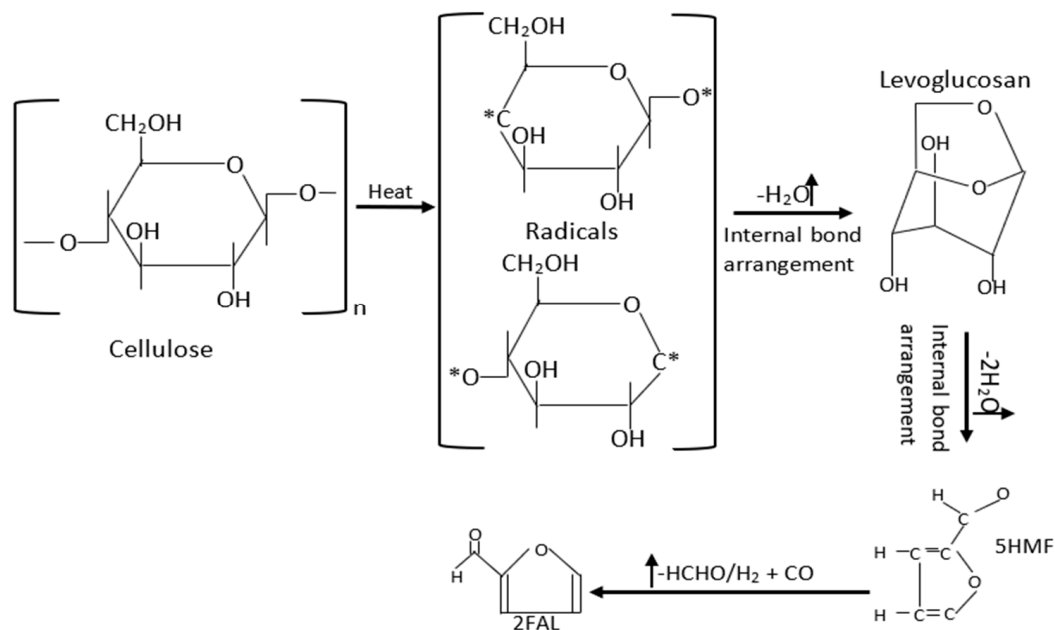


Figure 2. Hydrolysis mechanism in cellulose.



**Figure 3.** Pyrolysis mechanism in cellulose.

Recently, technology involving the enhancement of dielectric materials using nano-modification is now one of the trending areas in the materials dielectric field [55–57]. The initiation of nanoparticles majorly improves the mechanical and electrical performance of insulating components [58]. Cellulose insulating paper can be modified either by adding nanoparticles to the cellulose paper before impregnating it into insulating oil or by adding nanoparticles to the insulating oil to yield nanofluid and then impregnate the cellulose paper into the nanofluid [59]. Many works have therefore been done to actualize the enhancement of mechanical and electrical performance insulating paper with the aid of nanoparticles [60–63]. Numerous micron-level fillers have been used in the traditional paper industry to enhance paper performance. These fillers significantly decrease the mechanical properties of insulating paper as such, the fillers cannot be applied to modify the properties of insulating paper [64,65]. Therefore, the advent of nanotechnology has given rise to the use of nanoscale filler in paper-making industries and this has been reported to have considerable influence on the paper [66–68]. Nanoparticles used for modification have been divided into three types, which are insulating nanoparticles such as SiO<sub>2</sub>, BN, and Al<sub>2</sub>O<sub>3</sub>; semi-conductive nanoparticles such as SiC, CuO, TiO<sub>2</sub>, and ZrO<sub>2</sub>; and conductive nanoparticles such as Fe<sub>3</sub>O<sub>4</sub>, ZnO, Fe<sub>2</sub>O<sub>3</sub>, and graphene [69–71].

Materials from paper coated and cotton cloth were the foremost solid insulating materials used in power transformers. Due to the increase in the voltage level of power transformers, there was an emergence of Kraft-paper insulating oil in the 1920s [72]. A composite paper formed from polymer film and cellulose paper was introduced in the 1950s, which has a better dielectric performance relative to pristine cellulose paper [73]. Thermally upgraded Kraft (TUK) paper was introduced for use in power transformers because it decreases the cellulose rate of molecular chain scission, which impedes the loss of the tensile strength of the paper in power transformers in the course of ageing [74]. TUK paper, known as Nomex paper, was fabricated from Kraft paper in the course of paper pulping by making stable cyanoethyl groups to substitute hemicellulose and cellulose reactive OH groups through cyanoethylation [75]. The paper mechanical strength and hydrogen bridges in this modification are lessened and due to environmental issues, this approach was thereafter rejected [74,76]. A new approach involves the addition of melamine, polyacrylamide, dicyandiamide, and amide salts, which are all nitrogen-stabilizing agents in the last phase of paper-making, which interacts mainly with the surfaces of the paper. Here, cellulose oxidation is reduced as the weak bases from amide products interact with the

cellulose deterioration products, which partially consume moisture and neutralize the oil acidity. Furthermore, primary amides and part of the ammonia react with 2-furaldehyde (2FAL) to produce melanoidins and furfuralamide, which is the reason 2FAL content in TUK paper is very little [74,75]. Therefore, this modification decreases the cellulose ageing by three compared to typical Kraft paper because the cellulose ageing autocatalytic reactions are being impeded by the nitrogen stabilizing agent [75,76]. Diamond-dotted paper is fabricated from Kraft paper coated with thermosetting resin and is developed for high mechanical strength applications. The resin diamond-dotted paper ensures the paper is dried efficiently as it makes a large surface for bonding. Mineral oils, synthetic esters, and natural esters are the fluids used for liquid insulation. The addition of nanoparticles in a certain volume ratio to these oils proved to have enhanced the oil dielectric performance [77–80]. Although the consequence of nanoparticles on the cellulose of solid insulation has not been explored in detail, the cellulose of solid insulation has been said to have displayed an interaction between the fluid nanoparticles with which it was impregnated [81].

## 2. Chemical Indicators

The non-destructive assessment of the ageing conditions of power transformers without a power disconnection has been a topic of interest to researchers and engineers. The ageing state of cellulose paper used in transformer insulation can be characterized by monitoring the chemical indicators used in transformer oil [82,83]. However, transformer insulation conditions cannot be accurately assessed by a single chemical indicator since the concentration of these indicators generated depend on oxygen, moisture, and temperature [84,85]. The summary of the relationship between the concentration of chemical indicators, degree of polymerization, and condition of oil-paper insulation are given in Table 1 [86–90].

**Table 1.** Insulation condition based on chemical indicators concentration.

DP Value	2FAL (ppm)	MeOH (ppb)	CO <sub>2</sub> (ppm)	CO (ppm)	Oil-Paper State
1200–700	0–0.1	0–50	0–2500	0–350	Healthy insulation
700–450	0.1–1	51–200	2501–4000	351–570	Moderate degradation
450–250	1–10	201–250	4001–10,000	571–1400	Extensive degradation
<250	>10	>250	>10,000	>1400	End of useful life

### 2.1. CO and CO<sub>2</sub> Content

Oil-paper insulation undergoes a cracking and oxidation reaction under thermal stress, which generates a little oxide that then dissolves in the insulation oil [91]. CO and CO<sub>2</sub> gases are therefore a result of cellulose overheating. Their ratio shows a fault in insulation paper while leaving traces of carbon on it [92]. DGA (dissolve gas analysis) is used to determine the condition of paper insulation, and according to the ASTM D3612 standard, dissolved gases in the insulating oil can be collected through this analysis [93,94]. Certain combustible gas contents and their production rates are detected during DGA for transformer oils [45]. The ratio of CO<sub>2</sub> to CO in the transformer oil is used to diagnose the paper degree of polymerization, which yields more information on the paper insulation status. According to IEC 60599, for a paper in a normal ageing state, this ratio should be between 3 and 10 [3,95,96]. However, long-duration oxidation of insulating oil constituents and oxygen via leaks also generates oxides of carbon in which the ratio may be higher or lower than the stated values [3,97]. Therefore, the ratio of CO<sub>2</sub> to CO is not sufficient to diagnose the condition of paper insulation and its degree of polymerization [98].

He et al. [99] measured the CO<sub>2</sub> and CO concentration in thermally aged oil-impregnated pure and modified paper at 130 °C and 2%wt of Al<sub>2</sub>O<sub>3</sub> nanoparticles by the IEC 60567-2011 standard using gas chromatography. It was reported that the concentration of CO<sub>2</sub> and CO dissolved in the oil-impregnated pure paper is higher than the impregnated Al<sub>2</sub>O<sub>3</sub>-modified paper and becomes greater with ageing.

## 2.2. Furan Content

Furan's derivatives are generated from cellulose hydrolytic deterioration and pyrolysis of levoglucosan [40,100,101]. The concentration of derivatives of furan in insulating oil can be analyzed by employing the ASTM D3612 standard via Gas Chromatography-Mass Spectroscopy (GC/MS) [102], and furthermore by the ASTM D5837 and IEC 6118 standards via High-Performance Liquid Chromatography (HPLC) [3,103]. Furanic compounds in insulating oil rely on the cellulose and oil mass ratio [45]. In addition, the broken glycosidic bond fractions in the cellulose paper yield more information about the rate at which furanic derivatives are produced [104]. 2-Furfural (2FAL), 2-Acetyl furan (2ACF), 2-Fulfulol (2FOL), 5-Methyl-2-furfural (5MEF), 2-furic acid (2F), and 5-Hydroxy methyl-2-furfural (5HMF) are the derivatives of furan produced from deteriorated cellulose paper in insulating oil according to the IEC 61198 standard. The sources of furanic derivatives formation and their chemical structures are shown in Table 2 [105] and Figure 4 [35,40,106], respectively. Furan derivatives in insulating oil are said to be directly related to the degree of polymerization of the cellulose insulation paper [107,108]. Therefore, the relationship between the degree of polymerization and furan concentration is given by:

$$DP_v = \left( \frac{2FAL}{\lambda} \right)^{\frac{1}{\psi d}} \quad (1)$$

where 2FAL is the furfuraldehyde concentration in ppm,  $DP_v$  is the degree of polymerization,  $d$ ,  $\lambda$ , and  $\psi$  are the constants that are dependent on the type of cellulose paper and winding longitudinal thermal gradient [109,110]. 2FAL was used in this Equation (1) as an overall analysis of life assessment because it has more thermal stability and is more present in large amounts in insulating oil than other furanic compounds [111,112]. It can be produced through the oxidation and hydrolysis mechanisms presented in Figure 5 [25].

**Table 2.** Sources of furanic derivatives formation.

Furanic Derivatives	Sources
2FAL	Increase in temperature, normal ageing
5MEF	Excessive temperature
2ACF	Rare, no common cause
5HMF	Oxidation
2FOL	High moisture

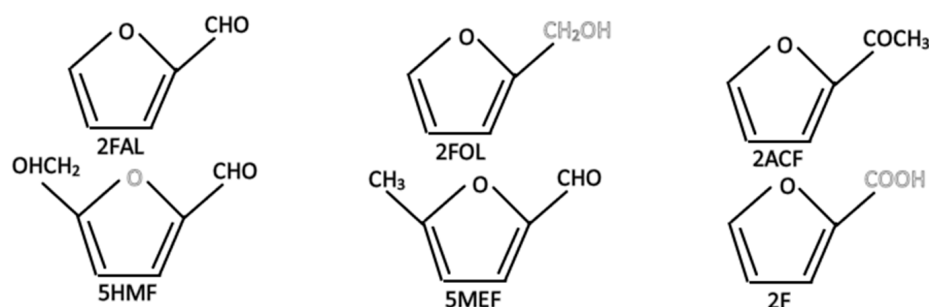


**Figure 4.** Chemical structure of furan derivatives.

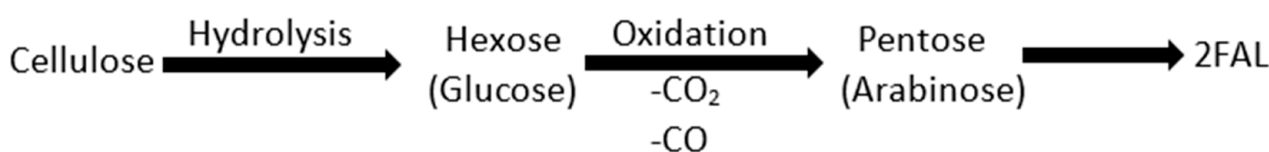


**Figure 5.** Production of 2FAL through cellulose hydrolysis and oxidation.

Ramazani et al. [113] measured the content of 2-furfural in oil-impregnated paper using HPLC according to the IEC 61198 standard. They established that 2FAL and 5HMF were the only furanic compounds detectable during accelerated pyrolysis of the cellulose. He et al. [99] measured the furfural concentration in thermally aged oil-impregnated pure and modified paper at 130 °C and 2%wt of Al<sub>2</sub>O<sub>3</sub> nanoparticles by the IEC 61198-1993 standard using a high liquid performance chromatography. It was reported that after 744 h, the furfural concentration in the oil-impregnated pure paper is 46.5% higher than the impregnated Al<sub>2</sub>O<sub>3</sub>-modified paper.

The addition of nitrogen stabilizing agents to normal Kraft paper to make thermally upgraded Kraft paper has limited the use of furans analysis for accessing paper's ageing condition as 2FAL is almost absent in aged thermally upgraded Kraft paper since some of these stabilizing agents (primary amides) react with 2FAL to produce melanoidins and furfamide [114]. Additionally, online analysis of furanic derivatives is not achievable [115] and there are diverging observations for various types of insulating fluids [116].

### 2.3. Methanol (MeOH) Content

The introduction of thermally upgraded paper, which is frequently used in new power transformer insulation, has made furan analysis less effective as this paper barely produces furan derivatives [117,118]. Furthermore, the concentration of furan in the insulating oil is only observable when the paper degree of polymerization is less than 400, which is a critical ageing stage of insulation paper [82]. Therefore, methanol has been discovered as one of the chemicals present in insulating oil of in-service power transformers and it also shows paper deterioration earlier than the furans [24,118–120]. The chain glycosidic bonds that hold the cellulose monomers break to generate a large amount of methanol [36,121]. Therefore, the scissions of glycosidic bonds in the cellulosic depolymerization chain vary directly as a result of the methanol generation [114,122]. Although ethanol is also present in insulating oil, its presence is particular to a system fault or as a result of higher temperatures in power transformers [120,123,124]. Therefore, methanol is a more effective chemical marker for the de-polymerization of insulation paper, as it does not depend on the type of cellulose paper since it is generated by all paper types and is very stable for any transformer working temperature [3,125].

Arroyo et al. [31] examined the tensile index and mechanical performance of thermally upgraded Kraft paper and standard Kraft paper using methanol as a chemical marker. They observed that methanol generation has a direct correlation with the number of scissions present in the cellulose chain and this number of scissions has shown a direct influence on the paper's mechanical performance.

## 3. Lifetime Model

Modeling the deterioration of insulation paper helps to foretell the time to replace a unit in power transformers to sustain the total reliability of this equipment. IEEE and IEC considered pyrolysis (temperature) among other factors that influence the rate of paper deterioration as a criterion for modeling ageing rate and end-of-useful life estimation [126]. IEEE proposed Equation (2) to determine the life lost as per [127,128]:

$$\%LL = \frac{F_{EQA} \times t \times 100}{\text{Normal insulation life}}, \quad (2)$$

$F_{EQA}$  can be computed by Equation (3) as:

$$F_{EQA} = \frac{\sum_{n=1}^N F_{AA,n} \Delta t_n}{\sum_{n=1}^N \Delta t_n}, \quad (3)$$

Additionally,  $F_{AA}$  is determined by Equation (4):

$$F_{AA} = e^{\left(\frac{15,000}{383} - \frac{15,000}{\theta_h} + 273\right)}. \quad (4)$$

$F_{AA}$  is the acceleratory factor,  $\theta_h$  is the hotspot temperature,  $\Delta t_n$  is the total time,  $F_{EQA}$  is the equivalent ageing factor, and %LL is the percent of life lost.

IEC also proposed Equations (5) and (6) as loss of life and paper rate of ageing, respectively [129].

$$L = \int_{t_1}^{t_2} V dt \text{ or } L \approx \sum_{n=1}^N V_n \times t_n. \quad (5)$$

$$V = 2^{\left(\frac{\theta_h - 98}{6}\right)}. \quad (6)$$

where  $\theta_h$  is the hotspot temperature,  $L$  is the loss of life,  $V$  is the paper rate of ageing, and  $t_n$  is the time between measurements.

However, IEC and IEEE fail to use hydrolysis (moisture content) and oxidation (oxygen) as criteria for their models. Therefore, to include these factors, model equations for life loss and degree of polymerization are proposed in [126], which are:

$$LL_n = \frac{t_n}{\left(\frac{1}{200} - \frac{1}{1000}\right) \times \frac{E_a}{A}} \times e^{\frac{E_a}{RT}}, \quad (7)$$

$$LL_t = 1 - \sum_{N=1}^N LL_n, \quad (8)$$

$$DP_n = \frac{1}{A \times t_n \times e^{\left(\frac{-E_a}{RT}\right)} + \frac{1}{DP_{n-1}}}. \quad (9)$$

where  $DP_n$  is the degree of polymerization after ageing period  $t_n$ ,  $DP_{n-1}$  is the paper degree of polymerization at the end of the last interval,  $R = 8.314 \text{ J/mol/K}$  is the ideal gas constant,  $T$  is the temperature in Kelvin,  $E_a$  is the activation energy in J/mol,  $LL_t$  is the total life lost after some time interval, which is usually the unity in the case of a new transformer and gradually reduces to zero,  $t_n$  is time-period, and  $LL_n$  is the life lost after the time-period.

$A$  is a unit of time reciprocal (per hour) and its value is computed from the oxygen and moisture content using Equations (10)–(12).

Low oxygen (<7000 ppm)

$$A = (1.78 \times 10^{12})w^2 + (1.10 \times 10^{10})w + 5.28 \times 10^7, \quad (10)$$

Medium oxygen (7000 ppm–14,000 ppm)

$$A = (2.07 \times 10^{12})w^2 + (5.61 \times 10^{10})w + 2.31 \times 10^8, \quad (11)$$

High oxygen (>16,500 ppm)

$$A = (2.99 \times 10^{12})w^2 + (9.78 \times 10^{10})w + 3.86 \times 10^8. \quad (12)$$

where  $w$  is the paper moisture content.

#### 4. Ageing Assessment

Diagnosis of the ageing condition is pertinent to power system security as the ageing of an oil-paper composite insulation system poses a direct danger to the transformer reliability [130,131]. Cellulose insulation in operation will undergo ageing, and the ageing rate is governed by different maintenance schemes and operational conditions of a power transformer. The degree of polymerization varies directly with the cellulose molecule's average length. Therefore, as the cellulose molecules are shortened by the effect of ageing, the degree of polymerization reduces significantly. New insulation has a degree of polymerization of more than 1200 but gradually reduces to about 200 to 300 as insulating paper approaches the end of its useful life [132–134]. Furthermore, based on ageing studies in laboratories, low molecular weight acid (LMA) has a dominant impact on acid-catalyzed

hydrolysis, which is said to be a principal factor that causes the ageing mechanism in paper insulation, among others, which could be pyrolysis and oxidation. This acid serves as an ageing accelerator in insulation paper [135–137].

#### 4.1. Post-Mortem Analysis

Most life models for power transformers are done by ageing experimental data in the laboratory but these models are not dependable, as the ageing parameters of an in-service transformer are sophisticated [44,138]. In addition, samples of insulation paper cannot be regularly collected from transformers in service compared to insulating oil samples [139]. Therefore, a post-mortem assessment of scrapped transformer is used to acquire details from the ageing of in-service paper and helps to reduce the data gap between in-service ageing and laboratory ageing [140,141].

#### 4.2. Acid Assessment

The presence of acids in oil-insulating paper improves insulation conductivity and causes corrosion of some metal parts, which leads to a temperature increase in localized regions [142]. They generate more organic acids and water due to  $H^+$  ions produced by them that enhance the hydrolysis of insulation paper [143]. High molecular weight acids (HMA), which are stearic and naphthenic acids, and low molecular weight acids (LMA), which are acetic, levulinic, and formic acids, are the two general types of oil-paper ageing acid by-products [144,145]. LMA is absorbed by insulation paper, but HMA is not absorbed by insulation paper but rather remains in the insulating oil [146]. Therefore, insulating paper deterioration is more noticeable in LMA than in HMA [147]. Measuring the acidity (LMA) in insulation paper has been an issue as there is no formalized measurement method. However, LMA, being a polar compound, can be collected from the insulation paper only by using a different polar compound such as water as a solvent according to the BS 62021 standard [148].

Zhang et al. [149] studied the effect of  $SiO_2$  nanoparticles on the diffusion of acid between the oil-paper interface. They observed that the presence of  $SiO_2$  nanoparticles in the insulating oil abated the acid diffusion as the results obtained from molecular dynamics simulation of centroid trajectory, density field distribution, and relative concentration reveal the presence of more acid in oil-paper modified with  $SiO_2$  nanoparticles than in a pristine oil-paper insulation system. This outcome was principally ascribed to an increase in adsorption energy and intermolecular hydrogen bonding of  $SiO_2$  nanoparticles to the acids where the number of hydrogen bonds between the paper and acid in the oil-paper modified with  $SiO_2$  nanoparticles is decreased by 32.5% relative to the pristine oil-paper insulation.

#### 4.3. Water Content

Pyrolysis of cellulose paper and inflow from surroundings are the main two sources of moisture formation [150]. Moisture diffuses into the insulating oil, which in turn improves its conductivity and as the temperature of the insulating oil increases, it causes the moisture to evaporate and float to form a bubble shape, which aids partial discharge activities and decreases the breakdown voltage [151]. It has been confirmed that insulating paper with 4% water content will undergo ageing four times quicker than dry insulating paper that has 0.5% water content [152], and also researchers have proved that increasing the water content twice will lead to a 50% decrease in paper insulation mechanical strength [153]. Frequency domain dielectric spectroscopy, cellulose-water adsorption isotherms, Karl Fischer titration, on-line water activity probes, return voltage measurement, and polarization and depolarization current measurements are the methods used to measure insulating paper water content [154,155].

A laboratory examination of the water content in the insulation paper of a power transformer is almost not achievable as removing the paper insulation implies disassembling a whole fraction of the transformer insulation [3]. Therefore, cellulose adsorption isotherms through coulometric Karl Fischer titration is a common method used to analyze the water

content from the insulating oil sample taken from the power transformer [156]. However, this method has drawbacks due to the difficulties in actualizing the thermodynamic equilibrium between the insulating oil and paper, as well as the water solubility in the deteriorated insulating oil. Furthermore, the water content adsorbed by pressboard and insulating paper can be measured by dielectric response methods (frequency domain dielectric spectroscopy and polarization and depolarization current measurements). The methods require a total disconnection of the transformer from the power supply, and a current is also required to be measured in nano-amperes (nA), but the electrical noise in the substation could make this impossible. Moreover, pressboard spacers and the barriers' water content are measured by these methods, but the temperature of the pressboard spacers and barriers might be lesser than that of the insulation paper wrapped around the conductors. As a result, the water content obtained from these methods might be higher than the precise insulation paper's water content. Therefore, the correct details on the sizes and shapes of the spacers and barriers used must be well known [154,157]. Recovery voltage measurement as one of the dielectric response methods for measuring the moisture content of insulating pressboards could result in some setbacks as its measurement requires ambient environmental conditions (temperature range between 20 and 30 °C and relative humidity above 70%) to obtain a consistent result. In addition, the separation of some ageing and water content impacts the recovery voltage measurement and limits its application [158]. Water-activity probes immersed in insulating oil are another method used, where a capacitive film sensor is used to obtain temperature data and the water-activity is used in calculating the paper water content [159]. The probes estimate the operating transformer conditions as disconnection is not imperative based on the probe position. However, the position in power transformers where the probes are to be installed for an optimum result has been a major concern [157].

According to [160], the concentration of water in the paper is evaluated by Fessler's equation and the water-activity is given by Equation (13), where  $p_o(T)$  and  $p_v(T)$  can be estimated from Equations (14) and (15), respectively.

$$a_w = \frac{p_v(T)}{p_o(T)}, \quad (13)$$

$$p_o(T) = 0.00603 \times e^{\frac{17.502T}{240.97+T}}, \quad (14)$$

$$C = 2.173 \times 10^{-7} \times p_v(T)^{0.6685} \times e^{\frac{4725.6}{T+273}}. \quad (15)$$

$C$  is the cellulose insulation water content expressed as a fraction of the dry weight of the cellulose insulation.  $a_w$  is the water-activity and  $T$  is the temperature in °C, and  $p_o(T)$  in atm is the water vapour partial pressure that is above the pure water in the equilibrium.

It was noted in [161] that the degree of ageing principally influences the frequency domain spectroscopy at a low frequency when the water content is low, but high water content influences all frequency ranges. It was explained that oil-paper interface polarization plays a lead role at a low-frequency range. As the frequency increases, the polarization rate cannot balance with the alternating electric field rate. Therefore, steering polarization plays a lead role at a higher frequency. Daniel et al. [157] estimated the paper water content using water-activity probes and dielectric response methods. They proposed that the installed water-activity probes should be positioned at the top of the transformer as the temperature of the oil at the top is needed to evaluate the paper water content correctly. This was a result of paper tending to deteriorate more speedily at the top than at the bottom of the transformer winding.

#### 4.4. Degree of Polymerization

The degree of polymerization insulation paper is the average number of glucose rings (anhydro- $\beta$ -glucose monomers units) in each of its cellulose chains [162]. It is a dimensionless quantity that is used to evaluate the paper's state of health [163] and serves as the globally accepted chief indicator to examine transformer ageing condition [131,164]. The value of

the degree of polymerization discloses a good interrelationship between the mechanical strength, ageing product formation, and degradation of the insulation paper [165]. The relationships given by Equations (16) and (17) are established to estimate paper degree of polymerization from the concentration of furan derivatives in the oil and paper's elapsed life, respectively.

$$DP = \frac{\log(0.88 \times 2FAL) - 4.51}{-0.0035}. \quad (16)$$

where the furan concentration of 2FAL is in parts per billion [166].

$$\text{Elapsed life} = 20.5 \ln\left(\frac{1100}{DP}\right). \quad (17)$$

where DP is the degree of polymerization and elapsed life is in years [167].

#### 4.4.1. Viscometric Method

The degree of polymerization of cellulose paper can be measured by the viscometric method. The average viscometric degree of polymerization of insulating paper can be known by measuring the paper viscosity dissolved with cupriethylenediamine and a deionized water mixture via a Ubbelohde viscometer tube, and the specific viscosity is evaluated to obtain the paper degree of polymerization [168,169].

He et al. [99] worked on the degree of polymerization of thermally aged pure and modified paper at 130 °C and 2%wt of Al<sub>2</sub>O<sub>3</sub> nanoparticles by the ASTM D4243-99 standard. It was noted that the degree of polymerization measured by an NCY-2 automatic viscometer of the pure paper is 6.4% higher than the Al<sub>2</sub>O<sub>3</sub>-modified paper during the early ageing period. However, at the end of 744 h of ageing time, the degree of polymerization of the Al<sub>2</sub>O<sub>3</sub>-modified paper is 15.2% higher than the pure paper. Therefore, the rate of decomposition of the cellulose chain is lower in Al<sub>2</sub>O<sub>3</sub>-modified paper than the pure paper. Chen et al. [49] experimentally measured the degree of polymerization of insulating Kraft paper modified with cellulose nanocrystals using the viscosity method according to the ASTM D4243 and GB/T 1548-2004 standards. Their result reported that the measured degree of polymerization of paper modified with cellulose nanocrystals after an ageing period of 672 h is enhanced by 50.5% compared to pure insulating paper. Liang et al. [170] measured the degree of polymerization of insulating paper at 130 °C and 2%wt of Al<sub>2</sub>O<sub>3</sub> nanoparticles using an NCY-2 automatic viscometer according to the ASTM D4243-99 standard. It was found that the degree of polymerization of Al<sub>2</sub>O<sub>3</sub>-modified paper is 29.4% higher than the pristine paper after 56 days. This indicated that the rate of ageing is slower in Al<sub>2</sub>O<sub>3</sub>-modified paper.

#### 4.4.2. Optical Sensor Method

Munster et al. [171] worked on a novel optical sensor measurement, which is a new technological development that provides online and non-destructive determination of an insulating paper's degree of polymerization through specific evaluation of the insulation paper reflection spectrum inside the transformer. During the ageing of insulation papers, they display different optimal parameters. Therefore, this serves as the rudiment for this optical measurement, which is based on the principles of optical spectroscopy. The insulating paper is illuminated at the head of the sensor with a source of light through an optical fibre cable, and a different optical fibre cable collecting the reflected light then transfers it to an optical spectrometer. Figure 6 shows the optical reflection spectroscopy principle used in their work. In line with the well-known viscometric method by IEC 60540, in their work they also used 11 different insulation paper (Grade K with density of 0.75–0.85 g/cm<sup>3</sup> and 0.1 mm thickness) samples aged in different insulating liquids (mineral oils, synthetic esters, and natural esters) with different transformers designs and modes of operation. Furthermore, two ageing systems (homogeneous and heterogeneous ageing) were used to study the impact of insulation paper arrangement on the sensor measurement. In heterogeneous ageing, the insulation papers were layered in the insulating

fluid while in homogeneous ageing, individual insulation papers were uniformly aged. Results reported in their work through various ageing analyses and correlations show that the degree of polymerization values by the sensor measurement and according to the IEC 60540 value behave correspondingly. A study was also carried out on an insulating paper sample of a transformer in operation for more than 50 years to validate the degree of polymerization value obtained from the sensor. In this experiment, the results obtained from the laboratory by IEC 60540 were so close to 200 (between 211 and 193) while the sensor values (between 260 and 131), although showing good similarity, corresponded well with ageing theory, as lower values of degree of polymerization are anticipated on the low voltage part and also outer layer values were higher than that of the inner layers. Therefore, they concluded that the newly discovered optical sensor measurement yields more valid and accurate values than the values obtained using the viscometric method according to IEC 60540.

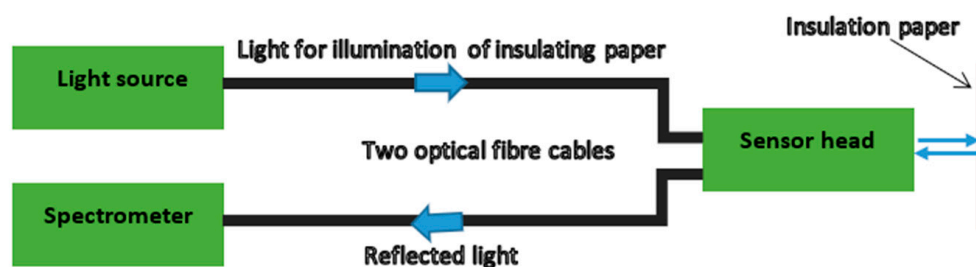


**Figure 6.** Insulation paper optical reflection spectroscopy principle.

#### 4.5. Tensile Strength

Tensile strength is defined as the capacity of a material to restrain damage when pulled. It has a direct relationship with the mechanical characteristics of insulating paper [172]. Paper strength is obtained from the inter-fibre covalent bonding strength and the fibre strength [173]. The end of useful life for paper insulation is given by IEEE and IEC to be 25% tensile strength retention. A decrease in tensile strength is determined by the loss of strength of the inter-fiber bond. The tensile strength and tensile index can be typically evaluated according to the BS 4415 standard using Equations (18) and (19), respectively [174].

$$TS = \frac{F}{w} \quad (18)$$

$$TI = \frac{TS}{g} \times 10^3 \quad (19)$$

where TS in kN/m, F in Newton, and w in mm denote tensile strength, maximum load, and paper width, respectively. Additionally, TI is the tensile index in N/mg, and gram-mage denoted by g is the ratio of paper weight to paper surface area measured in N/m<sup>2</sup>. According to [174], the paper degradation model as a function of time and temperature is given by the damage parameter as:

$$D = 1 - \frac{DP_i}{DP_o} \quad (20)$$

DP<sub>o</sub> is the paper's original DP value, DP<sub>i</sub> is the DP value after time and temperature ageing, and D is the parameter associated with paper damage. The damage D takes values between 0 and 1, where the D of value 1 corresponds to the total loss of Kraft paper mechanical strength while the D of value 0 represents fresh Kraft paper yet to undergo deterioration.

Liao et al. [65] investigated the tensile strength of softwood pulp insulating paper modified with TiO<sub>2</sub> nanoparticles at four different percentages by volume nanoparticles concentration. The tensile strength of the insulating paper was measured ten times for individual samples with the aid of AT-L-2, an ANMT instrument (electronic pull tester).

Their result was reported that the measured tensile strength in kN/m was reduced insignificantly relative to the pristine pulp paper by 0.23%, 1.03%, 0.35%, and 3.03% for 1%, 2%, 3%, and 4% TiO<sub>2</sub> volume concentrations, respectively. Yuan et al. [175] studied the effect of montmorillonite nanosheets on the tensile strength of oil-Kraft insulating paper using the ISO 1924-2:1994 standard. They reported a decrease in tensile strength with an increase in montmorillonite concentration and a remarkable decrement was experienced at a montmorillonite concentration beyond 9%. Hollertz et al. [176] compared the tensile strength of Kraft paper with nanofibrillated cellulose paper. In their work, the tensile strength index of nanofibrillated cellulose paper is 65% greater than the tensile strength index of the Kraft paper used. Chen et al. [49] experimentally examined the tensile strength of insulating Kraft paper modified with cellulose nanocrystals according to the ISO 1924-1 standard. Their result reported that the measured tensile index of Kraft paper reinforced with cellulose nanocrystals was improved by 17.3% compared to the pristine insulating paper. He et al. [99] measured the tensile strength of thermally aged pure and modified paper at 130 °C and 2%wt of Al<sub>2</sub>O<sub>3</sub> nanoparticles by the ISO 1924-2-2008 standard. It was reported that the tensile strength measured by the AL-L-1 tensile testing machine of the Al<sub>2</sub>O<sub>3</sub>-modified paper is greater than pure paper and this increases with ageing time. It was also observed that at the early ageing phase, both papers displayed an increase in tensile strength, and this occurrence was said to be a result of a further close connection between the cellulose chain due to thermal stress. During Al<sub>2</sub>O<sub>3</sub> nanoparticles modification, the alkoxide formed reacts with the hydroxyl of Al<sub>2</sub>O<sub>3</sub> nanoparticles surface, making the inorganic Al<sub>2</sub>O<sub>3</sub> nanoparticles surface organic. The cellulose chain and different organic functional groups were connected by the surface-modified Al<sub>2</sub>O<sub>3</sub> nanoparticles, which makes the cellulose chain closely connected and in turn, enhances the tensile strength of the composite paper. Xiang et al. [177] investigated the tensile strength of oil-impregnated insulation paper reinforced by Al<sub>2</sub>O<sub>3</sub> nanoparticles by the liquid doping method according to ISO1924-94 and GB/T12914-2008. The surface of the Al<sub>2</sub>O<sub>3</sub> nanoparticles was modified with a KH550 coupling agent. They reported that the tensile strength of Al<sub>2</sub>O<sub>3</sub>-modified paper improved by 16.7% compared to the pristine paper. Huang et al. [178] measured the tensile strength of insulating presspaper from softwood fiber reinforced at 10 wt% with unmodified nanofibrillated cellulose (UNFC), cationic nanofibrillated cellulose (CNFC), anionic nanofibrillated cellulose (ANFC), and cellulose nanocrystals (CNC) using the Zwick Z005 universal testing machine. This nano-cellulose is beneficial as being organic, it rarely needs surface modification and has more compatibility with insulating cellulose. In this work, they found that the tensile strength of presspaper reinforced by UNFC, CNFC, and ANFC increased by 8.26%, 24.77%, and 11.93%, respectively, while the tensile strength of presspaper reinforced by CNC decreased by 6.42% compared to the pristine pressboard. It was said that the density and Young modulus of the modified CNC pressboard and pristine presspaper are approximately equal, so this was not the major cause of the decrease in tensile strength of the presspaper modified with CNC. The tensile strength of the paper was explained to be a factor of individual fibres strength and interfibre bond strength, so the tensile strength was increased by decreasing softwood fibre content and increasing the concentration of CNC as it increased the effective number of fibres and enhanced the strength of the bond significantly. Furthermore, the discrepancy in tensile strength of CNFC- and ANFC-modified presspaper was said to be a result of the surface charge's polarity. The softwood fibers of the presspaper possess negative surface charges, which repel the negative surface charges of ANFC but attract the positive surface charges of CNFC. The electrostatic repulsion decreased the bond strength while electrostatic attraction enhanced the bond strength. Therefore, the polarity and size of the nano-cellulose are the major factors that influence the mechanical properties of nano-modified presspaper. Chen et al. [179] investigated the tensile strength of pressboard modified with SiC and Al<sub>2</sub>O<sub>3</sub> nanoparticles according to ISO 186:2002, ISO 1924:194, and ISO 1924-2-1994. Their result reported that the measured tensile strength in kN/m was moderately reduced relative to non-modified pressboard by 5%, and 13% for 2.5 wt% and 7.5 wt% Al<sub>2</sub>O<sub>3</sub> concentrations, respectively,

and 8% and 15% for 2.5 wt% and 7.5 wt% SiC concentrations, respectively. Perez-Rosa et al. [180] experimentally evaluated the tensile strength of Kraft paper impregnated with sunflower seed liquid (Bioelectra) modified with 0.1 g/L of Fe<sub>3</sub>O<sub>4</sub> nanoparticles using the MTC-100 vertical Universal Tensile Tester according to the ASTM D828-97 standard. They reported that the measured tensile strength of Kraft paper in Bioelectra reinforced with Fe<sub>3</sub>O<sub>4</sub> nanoparticles is slightly decreased compared to the Kraft paper in pure Bioelectra liquid. Although nanoparticles tend to reduce cellulose's mechanical properties, this slight loss can be neglected as both modified and un-modified samples have similar behaviour. Ibrahim et al. [181] measured the tensile strength of aged oil-impregnated Kraft paper modified with ZnO nanoparticles by an electronic testing instrument (10KN-LLOYD LR) according to the BS EN ISO 1924-2 standard. It was reported that the tensile strength of both modified and unmodified samples decreases slowly with ageing as a result of a decrease in polymer chain length caused by glycosidic inter-bonds breakage. At the early ageing stage, the unmodified sample shows a lesser decrease in tensile strength compared to the modified sample. However, at the end of the 336 h ageing period, the rate of tensile strength degradation in the modified sample is said to be 3% lower relative to the unmodified sample. The lower rate of degradation in the modified sample was accredited to ZnO nanoparticles' ability to dissipate heat easily and to absorb moisture during pyrolysis activity, which reduces the chemical bond breakage in the cellulose. Table 3 presents the summary of some cellulose paper tensile strength results after nanoparticles modification.

**Table 3.** Summary of tensile strength (TS) for some cellulose paper modified with nanoparticles.

Ref.	Year	Nanoparticle	Average Size	Particle Loading	Standard	Comment on TS
[65]	2013	TiO <sub>2</sub>	<60 nm	1% to 4% with 1% step	Not stated	Decreases slightly
[99]	2016	Al <sub>2</sub> O <sub>3</sub>	20 nm	2 wt% at 130 °C	ISO 1924-2-2008	Increases
[177]	2016	Al <sub>2</sub> O <sub>3</sub> + KH50	30 nm	Not stated	ISO 1924-94	Increases by 16.7%
[179]	2017	SiC/Al <sub>2</sub> O <sub>3</sub>	30 nm	2.5 wt% and 7.5 wt%	ISO 186:2002	Decreases moderately
[181]	2020	ZnO	<100 nm	Not stated	BS EN ISO 1924-2	Decreases by 3%
[180]	2022	Fe <sub>3</sub> O <sub>4</sub>	10 nm	0.1 g/L	ASTM D828-97	Decreases slightly

## 5. Electrical Properties

### 5.1. Dielectric Loss

Dielectric loss, also known as dissipation loss factor or  $\tan \delta$  in dielectric material, is caused by frictional loss as a result of the alignment of dipole–dipole or dipole–molecules interactions under alternating electric fields [182]. Furthermore, when an electric field is applied, there is a collision between electrons moving close to the anode and other molecules (dipoles and electrons), resulting in a loss of energy, thereby causing the material dielectric loss to be increased [183]. The dissipation factor of a material when placed in an electric field is the quantity of electrical energy that is said to dissipate in the form of heat, which increases the paper temperature during polarization [184]. It majorly relies on the electric field frequency and transformer power frequency [185]. Cellulose papers' dielectric performance principally depends on its chemical composition, the number of impurities, and crystallinity [186,187].

Liao et al. [65] measured the effect of TiO<sub>2</sub> nanoparticles on oil-impregnated insulation pulp paper at different frequencies using Novocontrol concept 80, GmbH, Germany (a broadband dielectric spectroscopy equipment). It was noted in this work that as frequency increases, they observed a decrease in dielectric loss of the oil-impregnated insulation paper. Furthermore, there was a decrease in dielectric loss as the concentration of TiO<sub>2</sub> nanoparticles increased. However, a significant decrease was observed at lower frequencies than at higher frequencies. Yan et al. [188] measured the dielectric loss of thermally aged oil-impregnated unbleached Kraft paper reinforced with 2 wt% of Al<sub>2</sub>O<sub>3</sub> nanoparticles at 130 °C. They confirmed that the dielectric loss of Al<sub>2</sub>O<sub>3</sub>-modified paper decreased by 42.4% compared to the pristine paper. Yuan et al. [175] worked on the effect of montmorillonite nanosheets on the dielectric loss of Kraft-oil insulation. The measured dielectric loss was done using a Novo control broadband dielectric spectrometer over a frequency range of

1 Hz to 10 MHz at an ambient temperature. They reported the optimal concentration of montmorillonite nanosheets to decrease the relative permittivity of the Kraft paper by 9.8% compared to the pristine Kraft paper. Oparanti et al. [189] experimentally measured the dielectric loss of palm kernel methyl ester-impregnated Kraft paper reinforced with  $\text{Al}_2\text{O}_3$  nanoparticles using the Rohde and Schwarz HM8118 LCR Bridge, Ontario, Canada according to the ASTM D1531 standard. They found that the dielectric loss of dry paper is lower than that of impregnated insulating paper. The report was said to be a result of discontinuity of charge mobility caused by micro-voids between the fibers of the dry paper. However, an increase in  $\text{Al}_2\text{O}_3$  nanoparticles in the pure sample leads to a decreased loss in the impregnated insulating paper. Cimbala et al. [190] found that at a high moisture content, the dielectric loss of pressboard impregnated in magnetic nanofluid was reduced by 50% relative to the pressboard impregnated in pristine oil. The reason for this reduction was as a result of nanoparticles being able to decrease the spreading of moisture in the insulating oil due to their hydrophilic nature. However, magnetic nanofluid conductivity has a significant effect on the dielectric loss of the insulating pressboard.

### 5.2. Breakdown Strength

Breakdown strength is the maximum field strength that insulating materials can resist to prevent a breakdown during electric field action. Insulation paper is placed between the upper and lower electrodes, voltage is then applied and increased to a particular value that causes paper insulation loss and damage [187]. Insulating oil-impregnated paper subjected to a high local electrical field causes streamers initiation as well as propagation that brings about the breakdown phenomenon [191–193].

Liao et al. [65] measured the breakdown strength of oil-impregnated insulation pulp paper modified by  $\text{TiO}_2$  nanoparticles at four different percentages by volume nanoparticles concentration using the IEC 60241:1998 standard. In this experiment, the breakdown strength of oil-impregnated insulation pulp paper was reported to have increased with an increased  $\text{TiO}_2$  concentration, with its optimal value at 3%  $\text{TiO}_2$  nanoparticles with a 20.83% increase relative to pristine oil-impregnated insulation pulp paper. A decrease in breakdown strength was recorded immediately after the 3% optimum concentration value. The obtained observation was explained to be a result of many gaps in the inner of an insulation paper. After impregnation, the gaps saturated with insulating oil undergo breakdown before any other parts as breakdown primarily takes place in the weakest part. Fast-moving electrons in the insulation system perhaps bring about the breakdown of oil-impregnated insulation paper. The introduced nanoparticles are present at the cellulose surface, as the nanoparticles enter the inner part of the insulation paper. These nanoparticles developed a trap area in the insulation system interfaces, and this reduces the velocity of the fast-moving electrons by continuous trapping and de-trapping in the trap area. Yuan et al. [175] worked on the effect of montmorillonite nanosheets on the breakdown voltage of Kraft-oil insulation. They reported that the optimal concentration of montmorillonite nanosheets improved the breakdown voltage of the insulation system by 13.1% relative to the pristine oil-paper insulation. Revathi et al. [194] examined the influence of  $\text{SiO}_2$  on the AC breakdown voltage of a 3 mm pressboard impregnated in mineral oil and rice bran oil. In their work, the breakdown voltage of 0.02% by volume of  $\text{SiO}_2$  in mineral oil-pressboard insulation improved by 6.25% compared to the pure mineral oil-pressboard insulation, while the breakdown voltage of 0.02% by volume of  $\text{SiO}_2$  in rice bran oil-pressboard insulation improved by 4.71% compared to the pristine rice bran oil-pressboard insulation. It was also observed that the pressboard impregnated in rice bran oil has a higher breakdown voltage than mineral oil. He et al. [99] measured the AC breakdown strength in kV/mm of oil-impregnated insulation paper modified with  $\text{Al}_2\text{O}_3$  nanoparticles at different concentrations according to IEC 60243-1. They reported an optimum breakdown strength at 2% by weight concentration of  $\text{Al}_2\text{O}_3$  nanoparticles, after which the breakdown strength decreased drastically. Xiang et al. [177] investigated the AC breakdown strength in kV/mm of oil-impregnated insulation paper reinforced by  $\text{Al}_2\text{O}_3$  nanoparticles by the

liquid doping method according to GB/T1408-2006. The surface of  $\text{Al}_2\text{O}_3$  nanoparticles was modified with a KH550 coupling agent. They found that the AC breakdown voltage  $\text{Al}_2\text{O}_3$ -modified paper improved by 17.2% compared to the pristine paper. Chen et al. [179] worked on the DC and AC breakdown strength of pressboard modified with SiC and  $\text{Al}_2\text{O}_3$  nanoparticles. They confirmed that the AC and DC breakdown strength of nano-modified pressboard initially increased and eventually decreased as the concentration of both SiC and  $\text{Al}_2\text{O}_3$  increased. They concluded that the optimal breakdown strength was observed at 2 wt% for both nanoparticles. However, the  $\text{Al}_2\text{O}_3$ -modified pressboard breakdown strength is higher than SiC-modified pressboard at all nanoparticles concentration. They attributed their result to the fact that the interface all around the nanoparticles is made up of two layers, which are the transition and bonded layers, that independently create shallow and deep traps. This trap serves fundamentally as the localized state that restrains ions in the forbidden band, making breakdown voltage improve with trap level. El-refaie et al. [195] investigated the influence of  $\text{Al}_2\text{O}_3$  nanoparticles on the AC breakdown voltage of pressboard impregnated in mineral oil. In their report, the breakdown voltage of 0.01 g/L, 0.04 g/L, 0.07 g/L, and 0.1 g/L of  $\text{Al}_2\text{O}_3$  in oil-pressboard insulation improved by 8.3%, 11.5%, 7.5%, and 3.9%, respectively, compared to the pure oil-pressboard insulation. They explained that as the insulating oil passes over the pressboard surface, there exists an interaction that leads to static electrification. Due to the interaction, the OH groups of the cellulose acquire a negative charge from the oil moving over them while the insulating oil is left with a positive charge since the surface on which the insulating oil travels determines the charge on it.  $\text{Al}_2\text{O}_3$  nanoparticles have OH groups on their surface caused by the natural absorbance of dissociated water, which makes them possess positive surface charge. Therefore, at a positive half cycle of the AC voltage applied, they have all their breakdown events. The improvement in their experiment was a result of  $\text{Al}_2\text{O}_3$  nanoparticles being able to hold the disassociation of negative charges as the principal reason for electrical discharge is the disassociated negative charge agglomeration. Therefore, the reduced breakdown strength at a higher weight fraction of  $\text{Al}_2\text{O}_3$  nanoparticles was connected to nanoparticles' agglomeration. Huang et al. [196] experimentally measured the DC positive and negative breakdown voltage of oil-impregnated insulation paper (0.12 mm thickness) modified with  $\text{TiO}_2$  nanoparticles at different concentrations according to IEC 60243 with 25 mm and 1 mm electrodes diameters and gaps, respectively. They found that the optimum breakdown voltage was noticed at 0.02 g/L  $\text{TiO}_2$  nanoparticles' concentration and the breakdown voltage reduces with an increase in concentration. The negative and positive breakdown voltage of oil-paper modified with  $\text{TiO}_2$  nanoparticles at 0.02 g/L was improved by 3.6% and 22.5%, respectively, compared to the unmodified oil-paper sample. They explained that negative voltage induces more interface charges as polarization currents under a positive voltage are lesser than that under a negative voltage. These charges accumulated at the interface under a negative voltage lessen the strength of the electric field in the sample, which makes a higher negative voltage necessary for breakdown, more so than a positive voltage. Liu et al. [197] worked on the breakdown voltage of oil-impregnated insulation paper (1 mm thickness) modified with  $\text{TiO}_2$  nanoparticles at different concentrations according to IEC 60243 under accelerated ageing at 158 °C. They found that the optimum breakdown voltage was noticed at 5 wt% of the  $\text{TiO}_2$  nanoparticles concentration. The nanoparticles have been said to have enhanced heat dissipation in the insulating paper. Shan et al. [198] experimentally studied the effect of  $\text{TiO}_2$  nanoparticles with a particle size of 5 nm on the negative DC breakdown voltage of oil-pressboard insulation according to ASTM D 149 and ASTM D 3755. They reported in this work that the negative DC breakdown voltage of oil-impregnated pressboard modified with  $\text{TiO}_2$  nanoparticles at 0.075% percentage concentration is increased by approximately 13% compared to the pristine sample. The nanoparticles decrease the charge injection quantity as a result of the enhanced charge injection of the Schokky potential barrier as well as the captured space charges accumulation that is weakened due to the reduction in deep trap density that favours a decrease in distortion of the electric field. Abd-Elhady et al. [199]

measured the AC breakdown strength of oil-impregnated insulation paper modified by three different nanoparticles with the same particle size of 25 nm. They found that the AC breakdown voltage of oil-paper modified by SiO<sub>2</sub>, Al<sub>2</sub>O<sub>3</sub>, and Pb<sub>3</sub>O<sub>4</sub> is maximally improved by 30%, 33%, and 37%, respectively, at 0.2 g/L concentration compared to the pristine oil-paper sample. The improved breakdown strength was explained to be due to the nanoparticles hydrophilic nature that helps to decrease the diffusion of moisture in insulation by absorbing the surface moisture content. In addition, more surface charge, which enhances free electrons that can be trapped, is held due to the high permittivity of nanoparticles. The result obtained shows that Pb<sub>3</sub>O<sub>4</sub> has a higher permittivity than SiO<sub>2</sub> and Al<sub>2</sub>O<sub>3</sub> nanoparticles. Du et al. [200] experimentally measured the DC and AC breakdown voltages of oil-paper modified with Fe<sub>3</sub>O<sub>4</sub> nanoparticles according to ASTM D3755 and ASTM D149, respectively. They reported that the optimal DC and AC breakdown voltages of Fe<sub>3</sub>O<sub>4</sub> oil-impregnated paper were improved by 10% and 9%, respectively, compared to the pure oil-impregnated paper sample. Perez-Rosa et al. [201] studied the AC breakdown voltage of oil-impregnated cellulose paper modified with 0.2 g/L concentrations of Fe<sub>3</sub>O<sub>4</sub> nanoparticles according to IEC 60243. They found that the AC breakdown voltage of the sample modified with Fe<sub>3</sub>O<sub>4</sub> nanoparticles is improved by 26% compared to the pristine sample. The improvement was said to be a result of a change in permittivity that caused the sample maximum electric field to decrease, thereby reducing the chances of streamer formation. Furthermore, streamer mobility was inhibited by nanoparticles as a result of charges accumulating around them. Table 4 presents the summary of some breakdown strengths of cellulose paper impregnated in nanofluid.

**Table 4.** Summary of breakdown strength of cellulose paper impregnated in nanofluid.

Ref.	Year	Nanoparticle	Average Size	Cellulose Material	Optimal Loading	Standard	Percentage Improvement
[65]	2013	TiO <sub>2</sub>	<60 nm	pulp paper	3 wt%	IEC 60241	+20.8% of DC BDV at 3 wt%
[194]	2015	SiO <sub>2</sub>	Not specified	pressboard	0.02%	Not specified	+6.25% AC BDV
[99]	2016	Al <sub>2</sub> O <sub>3</sub>	20 nm	pulp paper	2 wt%	IEC 60243	Increase in AC BDV
[177]	2016	Al <sub>2</sub> O <sub>3</sub> + KH50	30 nm	pulp paper	Not specified	GB/T1408	+17.2% AC BDV
[195]	2017	Al <sub>2</sub> O <sub>3</sub>	13 nm	pressboard	0.04 g/L	Not specified	+11.5% AC BDV
[196]	2021	TiO <sub>2</sub>	25 nm	Kraft paper	0.02 g/L	IEC 60243	+3.6% (negative) and +22.5% (positive) DC BDV
[198]	2019	TiO <sub>2</sub>	5 nm	pressboard	0.075 wt%	ASTM D149&D3755	+13% DC BDV
[199]	2021	Al <sub>2</sub> O <sub>3</sub> /SiO <sub>2</sub> /Pb <sub>3</sub> O <sub>4</sub>	25 nm	Kraft paper	0.2 g/L	ASTM	+33% (Al <sub>2</sub> O <sub>3</sub> ), +30% (SiO <sub>2</sub> ) and +30% (SiO <sub>2</sub> )
[200]	2020	Fe <sub>3</sub> O <sub>4</sub>	42 nm	Not specified	Not specified	ASTM D3755& D149	+10% (DC) and +10% (DC) and
[201]	2022	Fe <sub>3</sub> O <sub>4</sub>	10–15 nm	Kraft paper	0.2 g/L	IEC 60243	+26% (AC) BDV

### 5.3. Creeping Flashover Voltage

The weakest and most delicate insulation path is the oil-pressboard interface, which is a result of insulating oil and impregnated pressboard permittivity disparity [202]. When undergoing high electrical stress, sudden flashover or electrical breakdown is experienced due to surface streamers propagating with an approximated average velocity of 2 km/s [203,204]. The degradation of the pressboard surface structure can be caused by surface creeping discharges, which creates traces of carbon materials at the oil-pressboard interface. The applied voltage waveform, water level of solid substances, and localized electrical stress are used in detecting this creeping discharge [205–208]. There are four phases in an entire surface flashover process [209]. The centralized electric field at the oil-paper and electrode junction causes electron inception as a result of cathode field emission at the inception phase. With an increased applied voltage, the streamer traveled onward through the oil-paper interface at the streamer phase. The streamer moved toward the electrodes along the interface at the intermittent breakdown phase. Finally, at the surface flashover phase, a discharge channel is created and the bubbles in the oil are aroused, thereby degrading the paper surface [210–213]. Figure 7 shows the diagram used in carrying out a test on a creeping flashover test [214].

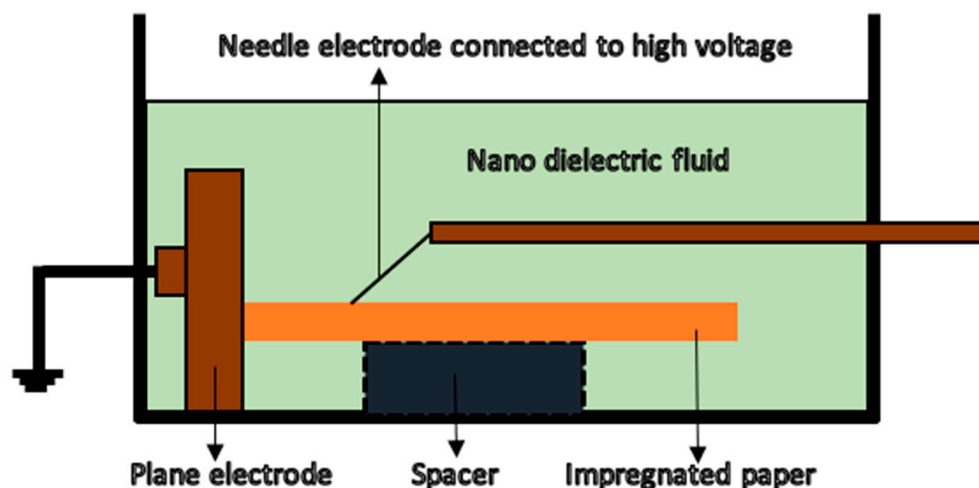


Figure 7. Set up for creeping flashover voltage test.

Ly et al. [215] worked on the effect of  $\text{TiO}_2$  nanoparticles on the oil-pressboard creeping flashover voltage under an AC electric field. They reported that the creeping flashover voltage of the  $\text{TiO}_2$  oil-pressboard interface is improved by 11.6% compared to the pristine oil-pressboard interface voltage. The presence of  $\text{TiO}_2$  nanoparticles was said to have resisted the surface discharge as the oil-pressboard surface space charge influenced the creeping flashover voltage. Furthermore, according to the electron scavenging model, nanoparticles can capture and turn fast-moving electrons in the insulating oil to slow-moving negative charges. The concentration of space charges at the oil-pressboard interface is connected to the surface creeping flashover. The streamers can move further as dissipation time for space charges is not sufficient. However, nanoparticles can help to speed up the rate of dissipation of the impregnated pressboard surface charge. This fast dissipation of surface charge can be accredited to the nanoparticles' ability to create a high and shallow trap density. The faster electrons captured hopping in the shallow traps created by nanoparticles are turned into slower electrons and are then quickly freed to the surrounding area. The authors also worked on negative and positive impulse creeping flashover voltages of oil-pressboard modified with  $\text{TiO}_2$  nanoparticles. At a 30 mm needle-plane electrode gap, the negative impulse and positive impulse creeping flashover voltages of  $\text{TiO}_2$  oil-pressboard were increased by 19.1% and 28.2%, respectively, compared to their respective pristine oil-pressboard voltages. It was observed that positive impulse creeping flashover showed a pronounced improvement over negative creeping flashover voltage and also the gap was directly proportional to the creeping flashover voltage. Abdul-Aleem et al. [216] investigated the creeping flashover voltage for oil-pressboard insulation modified with three nanoparticles ( $\text{SiO}_2$ ,  $\text{Al}_2\text{O}_3$ , and  $\text{Pb}_3\text{O}_4$ ) of the same particle size of 25 nm. It was reported that optimal enhancement was observed in oil-pressboard reinforced with  $\text{Pb}_3\text{O}_4$  nanoparticles as the maximum increase in oil-pressboard insulation reinforced with  $\text{SiO}_2$ ,  $\text{Al}_2\text{O}_3$ , and  $\text{Pb}_3\text{O}_4$ , was approximately 12%, 14%, and 23%, respectively, relative to the oil-pressboard insulation. Furthermore, they considered nanoparticles' concentration range of 0.1 g/L to 0.4 g/L and they confirmed that  $\text{SiO}_2$  and  $\text{Al}_2\text{O}_3$  have their optimal concentration value at 0.1 g/L while  $\text{Pb}_3\text{O}_4$  is at 0.2 g/L. It was explained that higher relative permittivity of  $\text{Pb}_3\text{O}_4$  nanoparticles compared to the relative permittivities of  $\text{SiO}_2$  and  $\text{Al}_2\text{O}_3$  nanoparticles were the principal reason for its maximum enhancement in oil-pressboard insulation. The high relative permittivity of nanoparticles enables high electrical field intensity at both interfaces of pressboard-nanoparticles and insulating oil-nanoparticles. Streamer charges are to a greater extent likely to stretch out in a zigzag manner as electric field intensity increases the streamer's force of attraction at the interface of oil-nanoparticles. Ge et al. [217] experimentally studied the surface flashover voltage for oil-impregnated paper-modified  $\text{TiO}_2$  nanoparticles. It was found that  $\text{TiO}_2$  oil-paper

insulation was enhanced by approximately 35% compared to pure oil-impregnated paper. It was said that the positive streamer's average velocity at the surface of the oil-impregnated paper was significantly changed by TiO<sub>2</sub> nanoparticles. The nanoparticles create more shallow traps, which help in fast dissipation of surface charges, and which decreases the accumulation of charge on the streamer tip as it restrains electric field distortion and reduces the streamers' propagation length. Therefore, streamers at the nanoparticles oil-impregnated paper surface find it difficult to develop, leading to improved surface flashover voltage. Huang et al. [218] examined the effect of TiO<sub>2</sub> nanoparticles with two different shapes on the creeping flashover voltage of an oil-impregnated 2 mm thick pressboard. The two shapes of TiO<sub>2</sub> used were spherical and rod-like, and were both rod-like with a diameter of 5 nm. They reported in this work that the creeping flashover voltage of 0.075 vol% spherical and rod-like TiO<sub>2</sub> oil-impregnated pressboard improved by 18.8% and 17.8%, respectively, compared to the reference oil-impregnated pressboard. They explained that creeping flashover is connected with the accumulation of space charge and its interface dissipation between the insulating oil and the pressboard. The accumulation and rate of dissipation of space charges are associated with trap densities and their corresponding energy levels. These trap densities are noticeably increased by the addition of both spherical and rod-like shape nanoparticles, which leads to the escape of charges from the shallow traps (created by the void on TiO<sub>2</sub> nanoparticles surface), which remarkably dissipate and decrease the accumulation of space charge on the nanofluid-impregnated pressboard surface. Large specific surface yields higher density and aids enough interaction between the two media. This makes the enhancement of the creeping flashover voltage in spherical shape nanoparticles to be more noticeable than in rod-like nanoparticles. Spherical shape nanoparticles have a specific surface area of about 1.3 times greater than rod-like nanoparticles. Therefore, spherical shape nanoparticles have shallow traps of higher density and lower energy levels. Shan et al. [219] experimentally investigated the effect of Fe<sub>3</sub>O<sub>4</sub> nanoparticles on the creeping flashover voltage of oil-pressboard insulation at three different electrode gaps under positive lightning impulse. It was found that at 0.2 g/L concentration of Fe<sub>3</sub>O<sub>4</sub> nanoparticles in the pristine oil-paper sample, the creeping flashover voltage was improved by 13.9%, 19.2%, and 15.8% at 20 mm, 30 mm, 40 mm electrode gaps, respectively, relative to the pristine sample. It was observed that at the three electrode gaps used in this work, the oil-paper modified with Fe<sub>3</sub>O<sub>4</sub> nanoparticles has shown high resistance to creeping discharge than the pristine oil-paper sample. The addition of Fe<sub>3</sub>O<sub>4</sub> nanoparticles noticeably increased the shallow trap density in the nanofluid/pressboard sample, which enhanced the surface charges mobility and prevented the accumulation of charges. El-Refaie et al. [220] investigated the flashover strength for oil-pressboard insulation modified with TiO<sub>2</sub> and Al<sub>2</sub>O<sub>3</sub> with particle sizes of 21 nm and 13 nm, respectively, at different flow conditions. At static conditions, it was reported that the optimal enhancement of flashover strength in oil-pressboard modified with TiO<sub>2</sub> and Al<sub>2</sub>O<sub>3</sub> nanoparticles was 11% and 8%, respectively, compared to the pristine sample. At dynamic flow conditions, the sample modified with Al<sub>2</sub>O<sub>3</sub> nanoparticles experiences a decrease in percentage improvement while the sample modified with TiO<sub>2</sub> nanoparticles shows an increase in percentage improvement. They concluded that the TiO<sub>2</sub> nanoparticles electron trapping capacity and Al<sub>2</sub>O<sub>3</sub> nanoparticles interface double layers enabled them to enhance the sample flashover strength under static conditions. The Al<sub>2</sub>O<sub>3</sub> nanoparticles interface double layer lost its effectiveness under dynamic flow conditions, which led to a decrease in percentage improvement.

#### 5.4. Partial Discharge

Partial discharge takes place in dielectric materials when the electric field exceeds the breakdown strength at a particular localized region, leading to discharges that partially bridge the dielectric insulation material between conductors [221,222]. It can be detected by ultra-high frequency sensors, optical fibre sensors, and piezo-electric sensors [223]. The lowest voltage that occurs as applied voltage is increased gives rise to partial discharge,

known as partial discharge inception voltage [224]. The activity of a partial discharge over a long period increasingly damages the insulating pressboard/paper as it creates conductive trees, which results in the failure of power transformers [225].

Lv et al. [215] studied the effect of TiO<sub>2</sub> nanoparticles on the partial discharge characteristics of oil-pressboard under an AC electric field. In their work, the partial discharge signals were monitored using a Doblelemke LDS-6 partial discharge detector device. The partial discharge inception voltage of a TiO<sub>2</sub> oil-pressboard is increased by 6% compared to the pristine oil-pressboard. Revathi et al. [194] examined the influence of SiO<sub>2</sub> nanoparticles on partial discharge inception voltage of a 3 mm pressboard impregnated in mineral oil and rice bran oil. In their work, the partial discharge inception voltage of 0.02% by volume of SiO<sub>2</sub> in mineral oil-pressboard insulation improved by 27.27% compared to the pure mineral oil-pressboard insulation, while a partial discharge inception voltage of 0.02% by volume of SiO<sub>2</sub> in rice bran oil-pressboard insulation improved by 10.61% compared to the pristine rice bran oil-pressboard insulation. It was also observed that the pressboard impregnated in rice bran oil has a higher partial discharge inception voltage than mineral oil. Huang et al. [218] examined the effect of TiO<sub>2</sub> nanoparticles with two different shapes on the partial discharge inception voltage of oil-impregnated 2 mm thick pressboard. The two shapes of TiO<sub>2</sub> used were spherical and 18 nm long and were both rod-like with a diameter of 5 nm. They confirmed in this work that the partial discharge inception voltage of 0.075 vol% spherical and rod-like TiO<sub>2</sub> oil-impregnated pressboard improved by 12.2% and 1.9%, respectively, compared to the reference oil-impregnated pressboard. They said that the shallow trap's lower energy level and higher density at the nanoparticles' interface significantly assisted dissipation of space charges and then decreased the space charge accumulation. Therefore, rod-like shape nanoparticles possess a steady charge twice that of spherical shape nanoparticles and a very slow charge dissipation rate, making its improvement insignificant. Liu et al. [226] experimentally studied the effect of TiO<sub>2</sub> nanoparticles with different diameters of 5 nm, 10 nm, 20 nm, and 30 nm on the partial discharge inception voltage of oil-paper insulation according to IEC 60243. In their work, the partial discharge inception voltage of the sample was observed to have an optimum value at TiO<sub>2</sub> with a particle size of 10 nm, with its partial discharge inception voltage enhanced by 22.8% compared to the pristine oil-pressboard sample. The enhanced value shows a decrease in the discharge channel on the surface of the insulating oil-paper sample, and this is due to the ability of the nanoparticles to fill the gaps between the cellulose.

### 5.5. Space Charge

Space charge brings about electrical field distribution distortion as it improves localized electrical stress, which has a remarkable influence on ageing, conductivity, and breakdown [227–229]. Insulation paper space charge behaviour depends mainly on the accumulated and dissipated charges. The enhanced behaviour of space charges is then considered to be less accumulation and faster dissipation of space charges [230,231]. An oil-paper insulation system's properties are in relationship with the space charge accumulated within oil-impregnated paper [232]. These accumulated space charges weaken or strengthen the localized field strength, and this can precede early failure in insulation in the case of the electric field strength being strengthened [233–235]. The dynamics of space charges in oil-paper insulation can be affected by water content, temperature, and voltage level [236]. Space charges can be in homo-polarized, hetero-polarized, and non-polarized dielectric interfaces. At the start of polarization, the amount of interfacial charge change in a homo-polarized interface is small, but there is a quicker increase in interfacial charge in a hetero-polarized interface than in a non-polarized interface [237]. In addition, by integrating the charge density, the total amount of charge trapped in oil-impregnated paper insulation can be found by [238,239].

$$Q(t) = \int_0^d |\rho(x, t)| S dx. \quad (21)$$

where  $d$  is the sample thickness in  $m$ ,  $\rho(x, t)$  is the sample internal charge density in  $C/m^3$ , and  $S$  is the electrode surface area in  $m^2$ .

Several materials such as Benzotriazole (BTA) have been used in oil-pressboards to enhance the behaviour of space charge due to their capacity to inhibit the charges accrued on the pressboard by shielding the surface charge adsorbed. However, superfluous molecules of BTA affect the insulating properties of the oil negatively. Therefore, insulating nanofluids by nanoparticles dispersion have been looked into [174].

Liao et al. [240] studied the internal electrical field and behaviour of space charge distribution in oil-impregnated paper insulation modified with semi-conductive  $TiO_2$  nanoparticles at two different concentrations of 1% and 3% detected by the pulsed electroacoustic (PEA) method. The maximum space charge density measured in  $C/m^3$  at 1% and 3%  $TiO_2$  nanoparticles was reported to have decreased by 29.9% and 55.1%, respectively, compared to the pure sample. The space charge density at the anode and cathode electrodes decreased and was irregular as stressing time increased. As detected by PEA when the electric field (DC) is applied, they explained the outcome of their result was a result of two different spaces charges, which are slow charges captured by deep traps and the fast charges captured by shallow traps. Therefore, the number of shallow traps indicates the number of fast charge. When the electric field is removed, PEA can only detect slow charges as fast charges are de-trapped and dissipated. Therefore, the amount of fast charges in space charges can be known by subtracting the amount of space charge when the field is removed from the amount of space charge of the oil-impregnated paper when the field is applied. The introduced nanoparticles created more shallow traps as well as converting some deep traps into shallow traps. This decreased the positive amount of space charge in the centre of oil-impregnated paper as well as increased the negative amount of space charge in oil-impregnated paper close to the cathode. Hollertz et al. [176] compared the space charge on pulp paper with nanofibrillated cellulose paper. In their work, the total space charge on nanofibrillated cellulose paper is 53.3% lesser than the total space charge on the pulp paper used. Liao et al. [241] investigated the influence of aluminum nitride (AlN) nanoparticles' surface coated with KH550 on cellulose paper space charge behaviour. A pulsed electroacoustic (PEA) instrument, which is made up of a digital oscilloscope, electroacoustic pulse measurement, DC voltage source, and impulse source, was employed to measure the space charge distribution. Semiconductor film was used to wrap the higher potential electrode (cathode) of the PEA instrument to obtain an improved acoustic match and the acoustic waves were identified and converted into electrical signals by a piezoelectric transducer fixed to the ground electrode (anode). They reported the charge injection inhibition effect according to paper space charge distribution by PEA to firstly improv and gradually diminish as AlN nanoparticles concentration increased from 0 wt% to 6 wt%. Furthermore, improvement of space charge behaviour was said to be more prominent in cellulose paper at 2 wt% AlN nanoparticles. It was noted that at 4 wt% to 60 wt% AlN concentration, more deep traps were present inside the cellulose paper, which has a detrimental consequence on dissipation and charge inhibition, while at 1 wt% and 2 wt% AlN concentration, more deep traps were present on the cellulose paper surface, which facilitates dissipation and charges inhibition. They also explained that AlN nanoparticles effect on cellulose paper space charge behaviour can be made clear using some facts about the trap in relationship with agglomeration and interfacial effects. Nanoparticles developed traps that moved to the surface of the paper as a result of the interfacial effect, which wipes out the shallow traps and more deep traps are formed due to the agglomeration. Thus, when the interfacial effect that leads to the migration of charge surpasses the agglomeration effect that leads to the generation of charge, the space charge behaviour of nano cellulose paper is enhanced. In cellulose paper, the interfacial effect takes place in the preeminent task as the whole performance of nano-modified paper is affected by competition between the interfacial effect and the agglomeration effect.

## 6. Challenges and Future Directions

The probability of adopting nanofluid in a few years to come is high due to the efforts and promising research output on nano-based fluids. However, the compatibility of these fluids with insulating cellulose paper has not been well examined. Among the pertinent areas of composite nanofluid-paper insulation systems that need proper and further investigations include:

Nano-structuring of solid/liquid materials to improve the reliability and performance of power equipment and to delay ageing, which is still of interest. Another important spin-off from this field of research concerns the optimization of voltage withstand, which should allow the design of more compact transformers. Indeed, the possibility of reducing the thickness of the insulating papers through the use of more efficient materials would make it possible to increase the conductor's size and consequently the power to be transported.

The effect of nanoparticles on insulation paper has been studied by many researchers. However, the evolutionary study of nanofluid-paper composite insulation should be given attention by the scientific community. In addition, investigation of the effect of surfactant used in nanofluid preparation on paper must be carefully examined.

The addition of nanoparticles has shown some diverging results on the tensile strength of insulation paper. Therefore, mechanical examination on the accelerated aged nanofluid-impregnated paper should be carefully investigated for better clarity on the strength and failure rate of the composite insulation system over a long time.

In a nanofluid-paper insulation system, infusion of fault is paramount to simulate the degassing tendency and the nature of gas generated by the composite insulation.

Corrective steps to be taken on a transformer are sometimes an issue as many reactions of solid/liquid insulation in transformers yield almost the same byproduct. Therefore, ambiguity set in when trying to identify the specific reaction that led to a particular fault. Researchers should give attention to these reactions by carrying out additional tests for exhaustive comprehension.

Online measurement of the degree of polymerization of insulation paper via an optical sensor to replace the offline measurement via the viscometric method is a new promising research area [174]. However, the use of this device is not yet generally accepted. Therefore, further study should be done on the use of the optical sensor method to validate and modify their proposed work for wide acceptance.

## 7. Conclusions

Insulation and cooling systems are very important to a power transformer's operational performance and life expectancy. Thus, proper monitoring of paper-oil composite insulation conditions is mandatory as an increase in moisture, temperature, and oxygen (air) accelerates insulation paper's hydrolytic, pyrolytic, and oxidative degradation, respectively. Nanoparticles added directly into insulation paper/oil display good enhancements on the electrical properties of the composite insulation and have to a large extent decreased the concentration of CO, CO<sub>2</sub>, methanol, and furanic compounds generated in the insulating fluid, which significantly reduced ageing activities. Although the degree of polymerization and tensile strength are parameters used in explaining the mechanical strength of paper insulation have shown a slight decrease with an increase in nanoparticles concentration, studies on insulation paper ageing have revealed that nano-modified paper subjected to ageing in terms of both temperature and time showed an improved degree of polymerization and tensile strength, compared to pristine paper throughout the ageing period. Mineral oil, which is the most used insulating oil in power transformers, has shown good compatibility with nano-impregnated paper. However, to mitigate the effect of environmentally unfriendly mineral oil, more studies need to be carried out on the compatibility of natural ester liquid with cellulose paper insulation.

**Author Contributions:** Conceptualization, A.A.A., S.O.O. and I.F.; methodology, A.A.A., S.O.O. and I.F.; validation, A.A.A., S.O.O. and I.F.; formal analysis, A.A.A.; investigation, A.A.A.; data curation, A.A.A., S.O.O. and I.F.; writing—original draft preparation, A.A.A., writing—review and editing, S.O.O. and I.F.; supervision, I.F.; project administration, I.F.; funding acquisition, I.F. All authors have read and agreed to the published version of the manuscript.

**Funding:** This research received no external funding.

**Data Availability Statement:** No data available for this work.

**Conflicts of Interest:** The authors declare no conflict of interest.

## References

1. Wang, Q.; Rafiq, M.; Lv, Y.; Li, C.; Yi, K. Preparation of Three Types of Transformer Oil-Based Nanofluids and Comparative Study on the Effect of Nanoparticle Concentrations on Insulating Property of Transformer Oil. *J. Nanotechnol.* **2016**, *2016*, 5802753. [[CrossRef](#)]
2. Morsalin, S.; Phung, T.B.; Danikas, M.; Mawad, D. Diagnostic challenges in dielectric loss assessment and interpretation: A review. *IET Sci. Meas. Technol.* **2019**, *13*, 767–782. [[CrossRef](#)]
3. Behjat, V.; Emadifar, R.; Pourhossein, M.; Rao, U.; Fofana, I.; Najjar, R. Improved Monitoring and Diagnosis of Transformer Solid Insulation Using Pertinent Chemical Indicators. *Energies* **2021**, *14*, 3977. [[CrossRef](#)]
4. Cong, H.; Pan, H.; Qian, D.; Zhao, H.; Li, Q. Reviews on sulphur corrosion phenomenon of the oil–paper insulating system in mineral oil transformer. *High Volt.* **2021**, *6*, 193–209. [[CrossRef](#)]
5. Tong, X.; Liang, Z.; Li, N.; Zhao, B.; Li, K.; Zhang, G. Comprehensive Analysis and Evaluation of Shandong Power Grid Station Automation Equipment. In Proceedings of the 2020 Asia Energy and Electrical Engineering Symposium (AEEES), Chengdu, China, 29–31 May 2020; pp. 632–637.
6. Metwally, I.A. Failures, Monitoring and New Trends of Power Transformers. *IEEE Potentials* **2011**, *30*, 36–43. [[CrossRef](#)]
7. Yu, S.; Zhao, D.; Chen, W.; Hou, H. Oil-immersed Power Transformer Internal Fault Diagnosis Research Based on Probabilistic Neural Network. *Procedia Comput. Sci.* **2016**, *83*, 1327–1331. [[CrossRef](#)]
8. Faiz, J.; Soleimani, M. Dissolved gas analysis evaluation in electric power transformers using conventional methods a review. *IEEE Trans. Dielectr. Electr. Insul.* **2017**, *24*, 1239–1248. [[CrossRef](#)]
9. El-Saied, H.; El-Meligy, M.G.; Mohamed, S.H.; Abd El-Mongy, S. Electrical insulated paper from cotton lint-er. *Carbohydr. Polym.* **2012**, *90*, 147–151. [[CrossRef](#)]
10. Coulibaly, M.-L.; Perrier, C.; Marugan, M.; Beroual, A. Aging behavior of cellulosic materials in presence of mineral oil and ester liquids under various conditions. *IEEE Trans. Dielectr. Electr. Insul.* **2013**, *20*, 1971–1976. [[CrossRef](#)]
11. Mishra, D.; Baral, A.; Haque, N.; Chakravorti, S. Condition Assessment of Power Transformer Insulation Using Short-Duration Time-Domain Dielectric Spectroscopy Measurement Data. *IEEE Trans. Instrum. Meas.* **2019**, *69*, 4404–4411. [[CrossRef](#)]
12. Maharana, M.; Baruah, N.; Nayak, S.K.; Sahoo, N. Comparative study of mechanical and electrical strength of kraft paper in nanofluid based transformer oil and mineral oil. In Proceedings of the 2017 International Symposium on Electrical Insulating Materials (ISEIM), Toyohashi, Japan, 11–15 September 2017; Volume 2, pp. 646–649.
13. Oparanti, S.O.; Salaudeen, I.K.; Adekunle, A.A.; Oteikwu, V.E.; Galadima, A.I.; Abdelmalik, A.A. Physico-chemical and Dielectric study on Nigerian Thevetia Peruviana as a potential green alternative fluid for transformer cooling/insulation. *Waste Biomass Valorization* **2022**, 1–11. [[CrossRef](#)]
14. Rao, U.M.; Fofana, I.; Rozga, P.; Picher, P.; Sarkar, D.K.; Karthikeyan, R. Influence of Gelling in Natural Esters Under Open Beaker Accelerated Thermal Aging. *IEEE Trans. Dielectr. Electr. Insul.* **2022**, *30*, 413–420. [[CrossRef](#)]
15. Madavan, R.; Balaraman, S. Comparison of antioxidant influence on mineral oil and natural ester properties under accelerated aging conditions. *IEEE Trans. Dielectr. Electr. Insul.* **2017**, *24*, 2800–2808. [[CrossRef](#)]
16. Soni, R.; Mehta, B. Review on asset management of power transformer by diagnosing incipient faults and faults identification using various testing methodologies. *Eng. Fail. Anal.* **2021**, *128*, 105634. [[CrossRef](#)]
17. Der Houhanessian, V. Measurement and Analysis of Dielectric Response in Oil-Paper Insulation Systems. Ph.D. Thesis, ETH Zurich, Zürich, Switzerland, 1998.
18. Tang, C.; Chen, G.; Fu, M.; Liao, R.-J. Space charge behavior in multi-layer oil-paper insulation under different DC voltages and temperatures. *IEEE Trans. Dielectr. Electr. Insul.* **2010**, *17*, 775–784. [[CrossRef](#)]
19. Setnescu, R.; Badicu, L.V.; Dumitran, L.M.; Notingher, P.V. Thermal lifetime of cellulose insulation material evaluated by an activation energy based method. *Cellulose* **2013**, *21*, 823–833. [[CrossRef](#)]
20. Fernández, I.; Delgado, F.; Ortiz, F.; Ortiz, A.; Fernández, C.; Renedo, C.J.; Santisteban, A. Thermal degradation assessment of Kraft paper in power transformers insulated with natural esters. *Appl. Therm. Eng.* **2016**, *104*, 129–138. [[CrossRef](#)]
21. Heathcote, M.J. *The J & P Transformer Book: A Practical Technology of the Power Transformer*; Newnes: London, UK, 1998.
22. Perez-Rosa, D.; Garcia, B.; Burgos, J.C. Dielectric Response of the Oil-Paper Insulation System in Nanofluid-Based Transformers. *IEEE Access* **2021**, *9*, 83797–83805. [[CrossRef](#)]

23. Zheng, Z.; Jin, Z.; Chen, L.; Chen, M.; Liu, J.; Yu, H.; Meng, Q.; Xie, P.; Xu, R. A comparative study of the ageing phenomena in Kraft paper and pressboard used in 500 kV class transformer. In Proceedings of the 2011 Annual Report Conference on Electrical Insulation and Dielectric Phenomena, Cancun, Mexico, 16–19 October 2011; pp. 620–623.
24. Abu Bakar, N.; Abu-Siada, A.; Islam, S. A review on chemical diagnosis techniques for transformer paper insulation degradation. In Proceedings of the 2013 Australasian Universities Power Engineering Conference (AUPEC), Hobart, TAS, Australia, 29 September–3 October 2013; pp. 1–6.
25. Tarasov, D.; Leitch, M.; Fatehi, P. Lignin–carbohydrate complexes: Properties, applications, analyses, and methods of extraction: A review. *Biotechnol. Biofuels* **2018**, *11*, 1–28. [[CrossRef](#)]
26. Arshad, M.; Islam, S.M. Significance of cellulose power transformer condition assessment. *IEEE Trans. Dielectr. Electr. Insul.* **2011**, *18*, 1591–1598. [[CrossRef](#)]
27. Zhou, H.; Long, Y.; Meng, A.; Li, Q.; Zhang, Y. The pyrolysis simulation of five biomass species by hemi-cellulose, cellulose and lignin based on thermogravimetric curves. *Thermochim. Acta* **2013**, *566*, 36–43. [[CrossRef](#)]
28. McShane, C.P.; Rapp, K.J.; Corkran, J.L.; Gauger, G.A.; Luksich, J. Aging of paper insulation in natural ester dielectric fluid. In Proceedings of the 2001 IEEE/PES Transmission and Distribution Conference and Exposition. Developing New Perspectives (Cat. No. 01CH37294), Atlanta, GA, USA, 2 November 2001; Volume 2, pp. 675–679.
29. Ese MH, G.; Liland, K.B.; Lesaint, C.; Kes, M. Esterification of low molecular weight acids in cellulose. *IEEE Trans. Dielectr. Electr. Insul.* **2014**, *21*, 662–665. [[CrossRef](#)]
30. Tang, C.; Zhang, S.; Xie, J.; Lv, C. Molecular simulation and experimental analysis of Al<sub>2</sub>O<sub>3</sub>-nanoparticle-modified insulation paper cellulose. *IEEE Trans. Dielectr. Electr. Insul.* **2017**, *24*, 1018–1026. [[CrossRef](#)]
31. Arroyo, O.H.; Jalbert, J.; Fofana, I.; Ryadi, M. Temperature dependence of methanol and the tensile strength of insulation paper: Kinetics of the changes of mechanical properties during ageing. *Cellulose* **2016**, *24*, 1031–1039. [[CrossRef](#)]
32. Abu-Siada, A.; Islam, S. A new approach to identify power transformer criticality and asset management decision based on dissolved gas-in-oil analysis. *IEEE Trans. Dielectr. Electr. Insul.* **2012**, *19*, 1007–1012. [[CrossRef](#)]
33. Dumitran, L.M.; Setnescu, R.; Notingher, P.V.; Badicu, L.V.; Setnescu, T. Method for lifetime estimation of power transformer mineral oil. *Fuel* **2014**, *117*, 756–762. [[CrossRef](#)]
34. Rodriguez-Celis, E.M.; Duchesne, S.; Jalbert, J.; Ryadi, M. Understanding ethanol versus methanol formation from insulating paper in power transformers. *Cellulose* **2015**, *22*, 3225–3236. [[CrossRef](#)]
35. Thiviyathan, V.A.; Ker, P.J.; Leong, Y.S.; Abdullah, F.; Ismail, A.; Jamaludin, M.Z. Power transformer insulation system: A review on the reactions, fault detection, challenges and future prospects. *Alex. Eng. J.* **2022**, *61*, 7697–7713. [[CrossRef](#)]
36. Arroyo, O.H.; Fofana, I.; Jalbert, J.; Ryadi, M. Relationships between methanol marker and mechanical performance of electrical insulation papers for power transformers under accelerated thermal aging. *IEEE Trans. Dielectr. Electr. Insul.* **2015**, *22*, 3625–3632. [[CrossRef](#)]
37. Liu, J.; Fan, X.; Zhang, Y.; Zheng, H.; Wang, Z.; Zhao, X. A Modified Aging Kinetics Model for Aging Condition Prediction of Transformer Polymer Insulation by Employing the Frequency Domain Spectroscopy. *Polymers* **2019**, *11*, 2082. [[CrossRef](#)]
38. Garcia, D.F.; Garcia, B.; Burgos, J.C. A review of moisture diffusion coefficients in transformer solid insulation-part 1: Coefficients for paper and pressboard. *IEEE Electr. Insul. Mag.* **2013**, *29*, 46–54. [[CrossRef](#)]
39. Azis, N. *Ageing Assessment of Insulation Paper with Consideration of In-Service Ageing and Natural Ester Application*; The University of Manchester: Manchester, UK, 2012.
40. Kaliappan, G.; Rengaraj, M. Aging assessment of transformer solid insulation: A review. *Mater. Today Proc.* **2021**, *47*, 272–277. [[CrossRef](#)]
41. Lelekakis, N.; Wijaya, J.; Martin, D.; Saha, T.; Susa, D.; Krause, C. Aging rate of grade 3 presspaper insulation used in power transformers. *IEEE Trans. Dielectr. Electr. Insul.* **2014**, *21*, 2355–2362. [[CrossRef](#)]
42. Koufakis, E.; Karagiannopoulos, C.; Bourkas, P. Thermal coefficient measurements of the insulation in distribution transformers of a 20kv network. *Measurement* **2008**, *41*, 10–19. [[CrossRef](#)]
43. Malik, H.; Yadav, A.K.; Mishra, S.; Mehto, T. Application of neuro-fuzzy scheme to investigate the winding insulation paper deterioration in oil-immersed power transformer. *Int. J. Electr. Power Energy Syst.* **2013**, *53*, 256–271. [[CrossRef](#)]
44. Baral, A.; Chakravorti, S. Condition assessment of cellulosic part in power transformer insulation using transfer function zero of modified debye model. *IEEE Trans. Dielectr. Electr. Insul.* **2014**, *21*, 2028–2036. [[CrossRef](#)]
45. Sun, H.-C.; Huang, Y.-C.; Huang, C.-M. A Review of Dissolved Gas Analysis in Power Transformers. *Energy Procedia* **2012**, *14*, 1220–1225. [[CrossRef](#)]
46. Ojewski, T.; Zięba, K.; Kołodziej, A.; Łojewska, J. Following cellulose depolymerization in paper: Comparison of size exclusion chromatography techniques. *Cellulose* **2011**, *18*, 1349–1363. [[CrossRef](#)]
47. Wang, M.; Cha, R. Industrialization progress of nanocellulose in China. *Pap. Biomater.* **2019**, *4*, 63–68.
48. Wang, D.; Liao, J.; Zhuo, R.; Liu, Z.; Xu, Y. Cantilever enhanced PA spectroscopy detection for CO decomposition in SF 6 equipment. In Proceedings of the 2022 IEEE 5th International Electrical and Energy Conference (CIEEC), Nangjing, China, 27–29 May 2022; pp. 3769–3774.
49. Chen, Q.; Kang, M.; Xie, Q.; Wang, J. Effect of melamine modified cellulose nanocrystals on the performance of oil-immersed transformer insulation paper. *Cellulose* **2020**, *27*, 7621–7636. [[CrossRef](#)]

50. Huaqiang, L.; Yanning, Z.; Lisheng, Z.; Qinxue, Y.; Xu, L.; Guangqi, L.; Mori, S.; Yamada, S. The DC breakdown of mineral insulating oil and oil-pressboard. In Proceedings of the 2013 Annual Report Conference on Electrical Insulation and Dielectric Phenomena, Shenzhen, China, 20–23 October 2013; pp. 929–931.
51. Zhang, M.; Liu, J.; Qi, P.; Chen, Q.; Liao, L.; Chen, X.; Yin, M. Measurement of dielectric response of transformer moisture content. *IET Sci. Meas. Technol.* **2018**, *12*, 594–602. [[CrossRef](#)]
52. Suleiman, A.A.; Muhamad, N.A.; Bashir, N.; Arief, Y.Z.; Rahman, M.N.A.; Phung, B.T. Moisture effect on conductivity of kraft paper immersed in power transformer vegetable-based insulation oils. *IET Gener. Transm. Distrib.* **2017**, *11*, 2269–2274. [[CrossRef](#)]
53. Zhu, M.; Liao, R.; Du, X.; Zhou, J.; Zhu, W. Simulation of diffusion of moisture in insulation paper and the effect on mechanical properties of the paper. *Trans. China Electrotech. Soc.* **2015**, *30*, 338–345.
54. Zaengl, W. Dielectric spectroscopy in time and frequency domain for HV power equipment. I. Theoretical considerations. *IEEE Electr. Insul. Mag.* **2003**, *19*, 5–19. [[CrossRef](#)]
55. Choudhary, S.; Sengwa, R.J. Morphological, structural, dielectric and electrical properties of PEO–ZnO nano-dielectric films. *J. Polym. Res.* **2017**, *24*, 54. [[CrossRef](#)]
56. Barrios, E.; Fox, D.; Li Sip, Y.Y.; Catarata, R.; Calderon, J.E.; Azim, N.; Afrin, S.; Zhang, Z.Y.; Zhai, L. Nanomaterials in Advanced, High-Performance Aerogel Composites: A Review. *Polymers* **2019**, *11*, 726. [[CrossRef](#)]
57. Yao, Y.; Zhao, F.; Wang, B.; Hu, Z.; Huang, Y. The designing of degradable unsaturated polyester based on selective cleavage activated hydrolysis and its application in recyclable carbon fiber composites. *Compos. Sci. Technol.* **2022**, *229*, 109692. [[CrossRef](#)]
58. Nazir, M.T.; Phung, B.T.; Zhang, Y.; Li, S. Dielectric and thermal properties of micro/nano boron nitride co-filled EPDM composites for high-voltage insulation. *Micro Nano Lett.* **2019**, *14*, 150–153. [[CrossRef](#)]
59. Zhang, S. The Micromechanism on the Doping Modification of Nano SiO<sub>2</sub> to the Oil-Immersed Cellulose Insulating Paper. Ph.D. Thesis, Southwest University, Chongqing, China, 2018.
60. Chan, K.-Y.; Yang, D.; Demir, B.; Mouritz, A.P.; Lin, H.; Jia, B.; Lau, K.-T. Boosting the electrical and mechanical properties of structural dielectric capacitor composites via gold nanoparticle doping. *Compos. Part B Eng.* **2019**, *178*, 107480. [[CrossRef](#)]
61. Lv, C. Study on the Preparation and Properties of Cellulose Insulation Paper Modified by Nano-TiO<sub>2</sub>. Ph.D. Thesis, Chongqing University, Chongqing, China, 2014.
62. Wang, Q.; Zhou, Y.; Chen, X. Effect of TiO<sub>2</sub> nanoparticles on surface discharge characteristics of transformer oil impregnated pressboard. *Insul. Mater.* **2015**, *48*, 36–40.
63. Liao, R.; Lv, C.; Wu, W.Q.; Liang, N.C.; Yang, L.J. Insulating properties of insulation paper modified by nano-Al<sub>2</sub>O<sub>3</sub> for power transformer. *J. Electr. Power Sci. Technol.* **2014**, *9*, 3–7.
64. Shen, J.; Song, Z.; Qian, X.; Ni, Y. A Review on Use of Fillers in Cellulosic Paper for Functional Applications. *Ind. Eng. Chem. Res.* **2011**, *50*, 661–666. [[CrossRef](#)]
65. Liao, R.; Lv, C.; Yang, L.; Zhang, Y.; Wu, W.; Tang, C. The insulation properties of oil-impregnated insulation paper reinforced with nano-TiO<sub>2</sub>. *J. Nanomater.* **2013**, *2013*, 1. [[CrossRef](#)]
66. Zhang, Y.; Zhang, L.; Cui, K.; Ge, S.; Cheng, X.; Yan, M.; Yu, J.; Liu, H. Flexible electronics based on micro/nanostructured paper. *Adv. Mater.* **2018**, *30*, 1801588. [[CrossRef](#)]
67. Momen, G.; Farzaneh, M. Survey of micro/nano filler use to improve silicone rubber for outdoor insulators. *Rev. Adv. Mater. Sci.* **2011**, *27*, 1–13.
68. Sethi, J.; Oksman, K.; Illikainen, M.; Sirviö, J.A. Sonication-assisted surface modification method to expedite the water removal from cellulose nanofibers for use in nanopapers and paper making. *Carbohydr. Polym.* **2018**, *197*, 92–99. [[CrossRef](#)]
69. Adekunle, A.; Oparanti, S. A Review on Physicochemical and Electrical Performance of Vegetable Oil-Based Nanofluids for High Voltage Equipment. *Electr. Power Syst. Res.* **2023**, *214*, 108873. [[CrossRef](#)]
70. Sima, W.; Shi, J.; Yang, Q.; Huang, S.; Cao, X. Effects of conductivity and permittivity of nanoparticle on transformer oil insulation performance: Experiment and theory. *IEEE Trans. Dielectr. Electr. Insul.* **2015**, *22*, 380–390. [[CrossRef](#)]
71. Primo, V.A.; Pérez-Rosa, D.; García, B.; Cabanelas, J.C. Evaluation of the Stability of Dielectric Nanofluids for Use in Transformers under Real Operating Conditions. *Nanomaterials* **2019**, *9*, 143. [[CrossRef](#)]
72. Prevost, T.A.; Oommen, T.V. Cellulose insulation in oil-filled power transformers: Part I-history and development. *IEEE Electr. Insul. Mag.* **2006**, *22*, 28–35. [[CrossRef](#)]
73. Shayesteh-Zeraati, A. *Synthesis of Multifunctional One-Dimensional and Two-Dimensional Highly Conductive Nano-Materials for Charge Storage Applications*; University of Calgary: Calgary, AB, Canada, 2020. [[CrossRef](#)]
74. Mildemberger, L.; Andreoli, M.C.; Silva GC, D.; Motta HN, D.; Gulmine, J.V.; Munaro, M. Correlation between stabilizer consumption and degree of polymerization of thermally upgraded paper aged in insulating natural ester and insulating mineral oil. *Polímeros* **2016**, *26*, 61–65. [[CrossRef](#)]
75. Lundgaard, L.E.; Hansen, W.; Linhjell, D.; Painter, T.J. Aging of oil-impregnated paper in power transformers. *IEEE Trans. Power Deliv.* **2004**, *19*, 230–239. [[CrossRef](#)]
76. Prevost, T.A. Thermally upgraded insulation in transformers. In Proceedings of the Electrical Insulation Conference and Electrical Manufacturing Expo, Indianapolis, IN, USA, 23–26 October 2005; pp. 120–125.
77. Primo, V.A.; García, B.; Burgos, J.C.; Pérez-Rosa, D. Investigation of the Lightning Impulse Breakdown Voltage of Mineral Oil based Fe<sub>3</sub>O<sub>4</sub> Nanofluids. *Coatings* **2019**, *9*, 799. [[CrossRef](#)]

78. Dai, J.; Dong, M.; Li, Y.; Zhou, J.; Wen, F. Influence of nanoparticle concentration on the frequency domain spectroscopy properties of transformer oil-based nanofluids. In Proceedings of the 2016 IEEE Conference on Electrical Insulation and Dielectric Phenomena (CEIDP), Toronto, ON, Canada, 16–19 October 2016; pp. 587–590.
79. Du, Y.; Lv, Y.; Li, C.; Chen, M.; Zhong, Y.; Zhou, J.; Li, X.; Zhou, Y. Effect of semiconductive nanoparticles on insulating performances of transformer oil. *IEEE Trans. Dielectr. Electr. Insul.* **2012**, *19*, 770–776. [[CrossRef](#)]
80. Zerinç, S.; Kakaç, S.; Yazıcıoğlu, A.G. Enhanced thermal conductivity of nanofluids: A state-of-the-art review. *Microfluid. Nanofluidics* **2010**, *8*, 145–170. [[CrossRef](#)]
81. Pérez-Rosa, D.; García, B.; Burgos, J.C.; Febrero, A. Morphological analysis of transformer Kraft paper impregnated with dielectric nanofluids. *Cellulose* **2020**, *27*, 8963–8975. [[CrossRef](#)]
82. N'Cho, J.S.; Fofana, I.; Hadjadj, Y.; Beroual, A. Review of Physicochemical-Based Diagnostic Techniques for Assessing Insulation Condition in Aged Transformers. *Energies* **2016**, *9*, 367. [[CrossRef](#)]
83. Zhang, E.; Zheng, H.; Zhang, C.; Wang, J.; Shi, K.; Guo, J.; Schwarz, H.; Zhang, C. Aging state assessment of transformer cellulosic paper insulation using multivariate chemical indicators. *Cellulose* **2021**, *28*, 2445–2460. [[CrossRef](#)]
84. Carrascal, I.A.; Fernández-Diego, C.; Casado, J.A.; Diego, S.; Fernández, I.; Ortiz, A. Quantification of Kraft paper ageing in mineral oil impregnated insulation systems through mechanical characterization. *Cellulose* **2018**, *25*, 3583–3594. [[CrossRef](#)]
85. Fernández-Diego, C.; Ortiz, A.; Carrascal, I.A.; Fernández, I.; Renedo, C.J.; Delgado, F.; Diego, S. Damage assessment of transformer Kraft paper insulation aged in mineral and vegetable oils. *Cellulose* **2019**, *26*, 2653–2672. [[CrossRef](#)]
86. Aciu, A.-M.; Nitu, M.C.; Nicola, M.; Nicola, C.-I.; Lazarescu, F. Complementary analysis of the degree of polymerization based on chemical markers 2-furaldehyde and methanol using the fuzzy logic. In Proceedings of the 2020 21st International Symposium on Electrical Apparatus & Technologies (SIELA), Bourgas, Bulgaria, 3–6 June 2020; pp. 1–6.
87. van Bolhuis, J.; Gulski, E.; Smit, J. Monitoring and diagnostic of transformer solid insulation. *IEEE Trans. Power Deliv.* **2002**, *17*, 528–536. [[CrossRef](#)]
88. Saha, T.K. Review of modern diagnostic techniques for assessing insulation condition in aged transformers. *IEEE Trans. Dielectr. Electr. Insul.* **2003**, *10*, 903–917. [[CrossRef](#)]
89. Abu-Siada, A.; Islam, S.; Lai, S. Remnant Life Estimation of Power Transformer using Oil UV-Vis Spectral Response. In Proceedings of the IEEE PES Power Systems Conference & Exhibition (PSC), Seattle, WA, USA, 15–20 March 2009; pp. 1–5.
90. Stevens, G.C.; Herman, H.; Baird, P. Insulation condition assessment through spectroscopic and chemometrics analysis. In Proceedings of the 2007 IEEE International Conference on Solid Dielectrics, Winchester, UK, 8–13 July 2007; pp. 717–720.
91. Srivastava, R.; Kumar, Y.; Banerjee, S.; Kale, S.N. Real-time transformer oil monitoring using planar frequency-based sensor. *Sens. Actuators A Phys.* **2022**, *347*, 113892. [[CrossRef](#)]
92. Prasojo, R.A.; Suwarno, S. Power Transformer Paper Insulation Assessment based on Oil Measurement Data using SVM-Classifer. *Int. J. Electr. Eng. Inform.* **2018**, *10*, 661–673. [[CrossRef](#)]
93. Bakar, N.A.; Abu-Siada, A.; Islam, S. A review of dissolved gas analysis measurement and interpretation techniques. *IEEE Electr. Insul. Mag.* **2014**, *30*, 39–49. [[CrossRef](#)]
94. Malik, H.; Tarkeshwar, J.; Jarial, R. Make Use of DGA to Carry Out the Transformer Oil-Immersed Paper Deterioration Condition Estimation with Fuzzy-Logic. *Procedia Eng.* **2012**, *30*, 569–576. [[CrossRef](#)]
95. Ghoneim, S. The Degree of Polymerization in a Prediction Model of Insulating Paper and the Remaining Life of Power Transformers. *Energies* **2021**, *14*, 670. [[CrossRef](#)]
96. Zhang, E.; Zheng, H.; Zhang, Y.; Liu, J.; Shi, Z.; Shi, K.; Zhang, C.; Shao, G.; Zhang, C.; Schwarz, H. Lifespan Model of the Relationships between Ethanol Indicator and Degree of Polymerization of Transformer Paper Insulation. *IEEE Trans. Dielectr. Electr. Insul.* **2021**, *28*, 1859–1866. [[CrossRef](#)]
97. Dessouky, S.S.; Kalas, A.E.; Abd El-Aal, R.A.; Hassan, A.M.M. Study and examination of transformer oil while exposed to air during operation. In Proceedings of the 2017 Nineteenth International Middle East Power Systems Conference (MEPCON), Cairo, Egypt, 19–21 December 2017; pp. 445–450.
98. Jalbert, J.; Rodriguez-Celis, E.; Duchesne, S.; Morin, B.; Ryadi, M.; Gilbert, R. Kinetics of the production of chain-end groups and methanol from the depolymerization of cellulose during the ageing of paper/oil systems. Part 3: Extension of the study under temperature conditions over 120 °C. *Cellulose* **2014**, *22*, 829–848. [[CrossRef](#)]
99. He, L.; Liao, R.; Lv, Y.; Yang, L.; Zhao, X.; Yan, S. Effect of nano-Al<sub>2</sub>O<sub>3</sub> on the thermal aging phys-icochemical properties of insulating paper. In Proceedings of the 2016 International Conference on Condition Monitoring and Diagnosis (CMD), Xi'an, China, 25–28 September 2016; pp. 254–257.
100. Scheirs, J.; Camino, G.; Avidano, M.; Tumiatti, W. Origin of furanic compounds in thermal deg radation of cel-lulosic insulating paper. *J. Appl. Polym. Sci.* **1998**, *69*, 2541–2547. [[CrossRef](#)]
101. Lelekakis, N.; Martin, D.; Wijaya, J. Ageing rate of paper insulation used in power transformers Part 1: Oil/paper system with low oxygen concentration. *IEEE Trans. Dielectr. Electr. Insul.* **2012**, *19*, 1999–2008. [[CrossRef](#)]
102. Cui, H.; Abu-Siada, A.; Li, S.; Islam, S. Correlation between dissolved gases and oil spectral response. In Proceedings of the 2017 1st International Conference on Electrical Materials and Power Equipment (ICEMPE), Xi'an, China, 14–17 May 2017; pp. 28–32.
103. ASTM D5837; Standard Test Method for Furanic Compounds in Electrical Insulating Liquids by High-Performance Liquid Chromatography (HPLC). ASTM International: West Conshohocken, PA, USA, 2015.

104. Zong, P.; Jiang, Y.; Tian, Y.; Li, J.; Yuan, M.; Ji, Y.; Chen, M.; Li, D.; Qiao, Y. Pyrolysis behavior and product distributions of bi-omass six group components: Starch, cellulose, hemicellulose, lignin, protein and oil. *Energy Convers. Manag.* **2020**, *216*, 112777. [[CrossRef](#)]
105. Thango, B.A.; Bokoro, P.N. Prediction of the Degree of Polymerization in Transformer Cellulose Insulation Using the Feedforward Backpropagation Artificial Neural Network. *Energies* **2022**, *15*, 4209. [[CrossRef](#)]
106. Pesavento, M.; Merli, D.; Biesuz, R.; Alberti, G.; Marchetti, S.; Milanese, C. A MIP-based low-cost electrochemical sensor for 2-furaldehyde detection in beverages. *Anal. Chim. Acta* **2020**, *1142*, 201–210. [[CrossRef](#)] [[PubMed](#)]
107. En-Wen, L.; Bin, S. Transformer health status evaluation model based on multi-feature factors. In Proceedings of the 2014 International Conference on Power System Technology, Chengdu, China, 20–22 October 2014; pp. 1417–1422.
108. Leibfried, T.; Jaya, M.; Majer, N.; Schafer, M.; Stach, M.; Voss, S. Postmortem investigation of power transformers—Profile of degree of polymerization and correlation with furan concentration in the oil. *IEEE Trans. Power Deliv.* **2013**, *28*, 886–893. [[CrossRef](#)]
109. Cheim, A.; Dupont, C. A new transformer aging model and its correlation to 2FAL. In *Cigré Transformer Colloquium*; CIGRE: Paris, France, 2003.
110. Cheim, L.; Platts, D.; Prevost, T.; Xu, S. Furan analysis for liquid power transformers. *IEEE Electr. Insul. Mag.* **2012**, *28*, 8–21. [[CrossRef](#)]
111. Teymouri, A.; Vahidi, B. Power transformer cellulosic insulation destruction assessment using a calculated index composed of CO, CO<sub>2</sub>, 2-Furfural, and Acetylene. *Cellulose* **2020**, *28*, 489–502. [[CrossRef](#)]
112. Talib, M.A.; Aziz, M.A.A.; Balasubramaniam, Y.; Ghazali, Y.Z.Y.; Abidin, M.R.Z.; Yousof, M.F.M. Transformer Ageing Investigation and Correlation of Furanic Compound and Degree of Polymerization for Power Transformer Life Assessment. In Proceedings of the 2020 IEEE International Conference on Power and Energy (PECon), Penang, Malaysia, 7–8 December 2020; pp. 240–244.
113. Ramazani, A.; Rahmati, R.; Bigdeli, S.; Rahmani, S.; Hamidi, M. *Aging Study of Transformer Oil-Impregnated Re-Pulped and Standard Cellulose by Measuring of 2-Furfural Content of the Oil*; ACECR, Scientific Information Database: Tehran, Iran, 2015.
114. Arroyo-Fernandez, O.H.; Fofana, I.; Jalbert, J.; Rodriguez, E.; Rodriguez, L.B.; Ryadi, M. Assessing changes in thermally upgraded papers with different nitrogen contents under accelerated aging. *IEEE Trans. Dielectr. Electr. Insul.* **2017**, *24*, 1829–1839. [[CrossRef](#)]
115. Meissner, M.; Darmann, M.; Schober, S.; Mittelbach, M.; Sumereder, C. Reliability Study of Furan Level Analysis for Transformer Health Prediction. In Proceedings of the 2019 IEEE 20th International Conference on Dielectric Liquids (ICDL), Roma, Italy, 23–27 June 2019; pp. 1–4.
116. Imani, M.T.; Homeier, K.; Werle, P.; Drager, G. How Far are Furan Compounds Reliable Indicators for Thermal Aging of Oil Impregnated Cellulose Insulation? In Proceedings of the 2018 IEEE Conference on Electrical Insulation and Dielectric Phenomena (CEIDP), Cancun, Mexico, 21–24 October 2018; pp. 438–441.
117. Shen, S. *Comparative Investigation on the Properties of Transformer-Used High Temperature Resistant Oil and Paper Insulation Materials*; POLITesi: Politecnico, Italy, 2016.
118. Jalbert, J.; Gilbert, R.; Denos, Y.; Gervais, P. Methanol: A novel approach to power transformer asset management. *IEEE Trans. Power Deliv.* **2012**, *27*, 514–520. [[CrossRef](#)]
119. Schaut, A.; Autru, S.; Eeckhoudt, S. Applicability of methanol as new marker for paper degradation in power transformers. *IEEE Trans. Dielectr. Electr. Insul.* **2011**, *18*, 533–540. [[CrossRef](#)]
120. Jalbert, J.; Rodriguez-Celis, E.M.; Arroyo-Fernández, O.H.; Duchesne, S.; Morin, B. Methanol marker for the detection of insulating paper degradation in transformer insulating oil. *Energies* **2019**, *12*, 3969. [[CrossRef](#)]
121. Fernández OH, A.; Fofana, I.; Jalbert, J.; Gagnon, S.; Rodriguez-Celis, E.; Duchesne, S.; Ryadi, M. Aging characterization of electrical insulation papers impregnated with synthetic ester and mineral oil: Correlations between mechanical properties, depolymerization and some chemical markers. *IEEE Trans. Dielectr. Electr. Insul.* **2018**, *25*, 217–227. [[CrossRef](#)]
122. Li, C.; Wu, K.; Li, Z.; Yang, Y.; Qian, K.; Kang, X. Effect of Electric Field on Methanol Generation in Transformer. In Proceedings of the 2018 IEEE Conference on Electrical Insulation and Dielectric Phenomena (CEIDP), Cancun, Mexico, 21–24 October 2018; pp. 382–385.
123. Li, S.; Ge, Z.; Abu-Siada, A.; Yang, L.; Li, S.; Wakimoto, K. A new technique to estimate the degree of polymerization of insulation paper using multiple aging parameters of transformer oil. *IEEE Access* **2019**, *7*, 157471–157479. [[CrossRef](#)]
124. Souza, E.M.P.V.S.; Mildemberger, L.; Akcelrud, L.; Andreoli, M.C.; Dos Santos, K.; Da Silva, G.C.; Da Motta, H.N.; Gulmine, J.V.; Munaro, M. Evaluation of the chemical stability of methanol generated during paper degradation in power transformers. *IEEE Trans. Dielectr. Electr. Insul.* **2016**, *23*, 3209–3214. [[CrossRef](#)]
125. Molavi, H.; Yousefpour, A.; Mirmostafa, A.; Sabzi, A.; Hamed, S.; Narimani, M.; Abdi, N. Static Headspace GC/MS Method for Determination of Methanol and Ethanol Contents, as the Degradation Markers of Solid Insulation Systems of Power Transformers. *Chromatographia* **2017**, *80*, 1129–1135. [[CrossRef](#)]
126. Martin, D.; Cui, Y.; Ekanayake, C.; Ma, H.; Saha, T. An updated model to determine the life remaining of transformer insulation. *IEEE Trans. Power Deliv.* **2014**, *30*, 395–402. [[CrossRef](#)]
127. C57.91-2011; IEEE Guide for Loading Mineral-Oil-Immersed Transformers and STP-Voltage Regulators. IEEE Standard: New York, NY, USA, 2012.
128. Godina, R.; Rodrigues, E.M.; Matias, J.C.; Catalão, J.P. Effect of loads and other key factors on oil-transformer ageing: Sustainability benefits and challenges. *Energies* **2015**, *8*, 12147–12186. [[CrossRef](#)]

129. IEC Central Office. *Power Transformers—Part 7: Loading Guide for Oil-Immersed Power Transformers*; IEC Central Office: Geneva, Switzerland, 2005.
130. Yang, D.; Chen, W.; Zhou, W.; Zou, J.; Fan, Z. Recognition of Aging Stage of Oil–Paper Insulation Based on Surface Enhanced Raman Scattering and Kernel Entropy Component Analysis. *IEEE Access* **2019**, *7*, 127862–127873. [[CrossRef](#)]
131. Yang, D.; Chen, W.; Wan, F.; Zhou, Y.; Wang, J. Identification of the Aging Stage of Transformer Oil–Paper Insulation via Raman Spectroscopic Characteristics. *IEEE Trans. Dielectr. Electr. Insul.* **2020**, *27*, 1770–1777. [[CrossRef](#)]
132. Krause, C. Power transformer insulation—history, technology and design. *IEEE Trans. Dielectr. Electr. Insul.* **2012**, *19*, 1941–1947. [[CrossRef](#)]
133. Duval, M.; De Pablo, A.; Atanasova-Hoehlein, I.; Grisaru, M. Significance and detection of very low degree of polymerization of paper in transformers. *IEEE Electr. Insul. Mag.* **2017**, *33*, 31–38. [[CrossRef](#)]
134. Liao, R.; Guo, C.; Wang, K.; Yang, L.; Grzybowski, S.; Sun, H. Investigation on thermal aging characteristics of vegetable oil–paper insulation with flowing dry air. *IEEE Trans. Dielectr. Electr. Insul.* **2013**, *20*, 1649–1658. [[CrossRef](#)]
135. Medina, R.D.; Romero, A.A.; Mombello, E.E.; Ratta, G. Assessing degradation of power transformer solid insulation considering thermal stress and moisture variation. *Electr. Power Syst. Res.* **2017**, *151*, 1–11. [[CrossRef](#)]
136. Kouassi, K.D.; Fofana, I.; Cissé, L.; Hadjadj, Y.; Yapi, K.M.L.; Diby, K.A. Impact of Low Molecular Weight Acids on Oil Impregnated Paper Insulation Degradation. *Energies* **2018**, *11*, 1465. [[CrossRef](#)]
137. Yao, W.; Li, J.; Huang, Z.; Li, X.; Xiang, C. Acids generated and influence on electrical lifetime of natural ester impregnated paper insulation. *IEEE Trans. Dielectr. Electr. Insul.* **2018**, *25*, 1904–1914. [[CrossRef](#)]
138. Aizpurua, J.I.; McArthur, S.D.; Stewart, B.G.; Lambert, B.; Cross, J.G.; Catterson, V.M. Adaptive power transformer lifetime predictions through machine learning and uncertainty modeling in nuclear power plants. *IEEE Trans. Ind. Electron.* **2018**, *66*, 4726–4737. [[CrossRef](#)]
139. Ghunem, R.A.; Assaleh, K.; El-Hag, A.H. Artificial neural networks with stepwise regression for predicting transformer oil furan content. *IEEE Trans. Dielectr. Electr. Insul.* **2012**, *19*, 414–420. [[CrossRef](#)]
140. Fernández-Diego, C.; Fernández, I.; Ortiz, F.; Carrascal, I.; Renedo, C.; Delgado, F. Assessment of dielectric paper degradation through mechanical characterisation. In *Simulation and Modelling of Electrical Insulation Weaknesses in Electrical Equipment*; IntechOpen: London, UK, 2018; p. 1.
141. Feng, D. *Life Expectancy Investigation of Transmission Power Transformers*; The University of Manchester: Manchester, UK, 2013.
142. Zhang, J.; Tang, C.; Qiu, Q.; Yang, L. Effect of water on the diffusion of small molecular weight acids in nano-SiO<sub>2</sub> modified insulating oil. *J. Mol. Liq.* **2020**, *314*, 113670. [[CrossRef](#)]
143. Frimpong, G.; Oommen, T.V.; Asano, R. A survey of aging characteristics of cellulose insulation in natural ester and mineral oil. *IEEE Electr. Insul. Mag.* **2011**, *27*, 36–48. [[CrossRef](#)]
144. Yan, Z.W.; Kihampa, T.; Matharage, S.Y.; Liu, Q.; Wang, Z.D. Measuring Low Molecular Weight Acids in Mineral and Ester Transformer Liquids. In Proceedings of the 2020 8th International Conference on Condition Monitoring and Diagnosis (CMD), Phuket, Thailand, 25–28 October 2020; pp. 354–357.
145. Lundgaard, L.E.; Hansen, W.; Ingebrigtsen, S. Ageing of Mineral Oil Impregnated Cellulose by Acid Catalysis. *IEEE Trans. Dielectr. Electr. Insul.* **2008**, *15*, 540–546. [[CrossRef](#)]
146. Zdemir, B.; Münster, T.; Werle, P.; Hämel, K.; Preusel, J. Investigations on Detectability of Different Acids in Paper–Oil Insulation. In Proceedings of the IET: 22nd International Symposium on High Voltage Engineering (ISH 2021), Hybrid Conference, Xi’an, China, 21–26 November 2021.
147. Venkatasubramanian, R.; Liu, Q.; Wang, Z.D.; Marshall, P. Assessment of regenerated oil through accelerated thermal ageing experiments. In Proceedings of the 2015 50th International Universities Power Engineering Conference (UPEC), Stoke on Trent, UK, 1–4 September 2015; pp. 1–4.
148. Allaf, H.N.; Mirzaei, H. Investigations on reclaimed oil performance through measurement of the relative free radical content. *IEEE Trans. Dielectr. Electr. Insul.* **2017**, *24*, 3481–3489. [[CrossRef](#)]
149. Zhang, J.; Tang, C.; Wang, Q.; Liu, X.; Du, D. Analysis of nano-SiO<sub>2</sub> affecting the acids diffusion in the interface between oil and cellulose paper. *Chem. Phys.* **2020**, *529*, 110557. [[CrossRef](#)]
150. Han, S.; Li, Q.; Li, C.; Yan, J. Electrical and mechanical properties of the oil–paper insulation under stress of the hot spot temperature. *IEEE Trans. Dielectr. Electr. Insul.* **2014**, *21*, 179–185. [[CrossRef](#)]
151. Jiang, J.P.; Du, B.X.; Cavallini, A. Effect of moisture migration on surface discharge on oil–pressboard of power transformers under cooling. *IEEE Trans. Dielectr. Electr. Insul.* **2020**, *27*, 1743–1751. [[CrossRef](#)]
152. Lelekakis, N.; Martin, D.; Wijaya, J. Ageing rate of paper insulation used in power transformers Part 2: Oil/paper system with medium and high oxygen concentration. *IEEE Trans. Dielectr. Electr. Insul.* **2012**, *19*, 2009–2018. [[CrossRef](#)]
153. Yin, F.; Tang, C.; Li, X.; Wang, X. Effect of Moisture on Mechanical Properties and Thermal Stability of Meta-Aramid Fiber Used in Insulating Paper. *Polymers* **2017**, *9*, 537. [[CrossRef](#)]
154. Martin, D.; Saha, T. A review of the techniques used by utilities to measure the water content of transformer insulation paper. *IEEE Electr. Insul. Mag.* **2017**, *33*, 8–16. [[CrossRef](#)]
155. Kierczynski, K.; Zukowski, P.; Sebok, M.; Gutten, M. Comparison of DC conductivity of the insulating oil and moisturized electrical pressboard impregnated with insulating oil. In *2018 ELEKTRO*; IEEE: Mikulov, Czech Republic, 2018; pp. 1–4.

156. Martin, D.; Saha, T.; Perkasa, C.; Lelekakis, N.; Gradnik, T. Fundamental concepts of using water activity probes to assess transformer insulation water content. *IEEE Electr. Insul. Mag.* **2016**, *32*, 9–16. [[CrossRef](#)]
157. Martin, D.; Saha, T.; Gray, T.; Wyper, K. Determining water in transformer paper insulation: Effect of measuring oil water activity at two different locations. *IEEE Electr. Insul. Mag.* **2015**, *31*, 18–25. [[CrossRef](#)]
158. Saha, T.K.; Yao, Z.T. Experience with return voltage measurements for assessing insulation conditions in service-aged transformers. *IEEE Trans. Power Deliv.* **2003**, *18*, 128–135. [[CrossRef](#)]
159. Martin, D.; Perkasa, C.; Lelekakis, N. Measuring Paper Water Content of Transformers: A New Approach Using Cellulose Isotherms in Nonequilibrium Conditions. *IEEE Trans. Power Deliv.* **2013**, *28*, 1433–1439. [[CrossRef](#)]
160. Mukherjee, M.; Martin, D.; Kulkarni, S.V.; Saha, T. A mathematical model to measure instantaneous moisture content in transformer insulation cellulose. *IEEE Trans. Dielectr. Electr. Insul.* **2017**, *24*, 3207–3216. [[CrossRef](#)]
161. Xia, G.; Wu, G.; Gao, B.; Yin, H.; Yang, F. A New Method for Evaluating Moisture Content and Aging Degree of Transformer Oil-Paper Insulation Based on Frequency Domain Spectroscopy. *Energies* **2017**, *10*, 1195. [[CrossRef](#)]
162. Teymouri, A.; Vahidi, B. CO<sub>2</sub>/CO concentration ratio: A complementary method for determining the degree of polymerization of power transformer paper insulation. *IEEE Electr. Insul. Mag.* **2017**, *33*, 24–30. [[CrossRef](#)]
163. IEC-60450; Measurement of the Average Viscometric Degree of Polymerization of New and Aged Cellulosic Electrically Insulating Materials. IEC: London, UK, 2004.
164. Wang, Y.; Gao, J.; Liao, R.; Zhang, Y.; Hao, J.; Liu, J.; Ma, Z. Investigation of characteristic parameters for condition evaluation of transformer oil-paper insulation using frequency domain spectroscopy. *Int. Trans. Electr. Energy Syst.* **2014**, *25*, 2921–2932. [[CrossRef](#)]
165. Tang, C.; Zhang, S.; Wang, X.; Hao, J. Enhanced mechanical properties and thermal stability of cellulose insulation paper achieved by doping with melamine-grafted nano-SiO<sub>2</sub>. *Cellulose* **2018**, *25*, 3619–3633. [[CrossRef](#)]
166. Martin, D.; Saha, T.; Dee, R.; Buckley, G.; Chinnarajan, S.; Caldwell, G.; Zhou, J.B.; Russell, G. Determining water in transformer paper insulation: Analyzing aging transformers. *IEEE Electr. Insul. Mag.* **2015**, *31*, 23–32. [[CrossRef](#)]
167. Gouda, O.E.; El Dein, A.Z. Prediction of Aged Transformer Oil and Paper Insulation. *Electr. Power Compon. Syst.* **2019**, *47*, 406–419. [[CrossRef](#)]
168. Oria, C.; Carrascal, I.; Ortiz, A.; Fernandez, I.; Ferreno, D.; Afshar, R.; Gamstedt, K. Experimental and numerical analysis of cellulosic insulation failures of continuously transposed conductors under short circuits and thermal ageing in power transformers. *IEEE Trans. Dielectr. Electr. Insul.* **2020**, *27*, 325–333. [[CrossRef](#)]
169. Fernández-Diego, C.; Carrascal, I.A.; Ortiz, A.; Fernández, I.; Ferreño, D.; Diego, S.; Casado, A. Fracture toughness as an alternative approach to quantify the ageing of insulation paper in oil. *Cellulose* **2021**, *28*, 11533–11550. [[CrossRef](#)]
170. Liang, N.; Liao, R.; Xiang, M.; Mo, Y.; Yuan, Y. Effect of Nano Al<sub>2</sub>O<sub>3</sub> Doping on Thermal Aging Properties of Oil-Paper Insulation. *Energies* **2018**, *11*, 1176. [[CrossRef](#)]
171. Münster, T.; Werle, P.; Peter, I.; Hämel, K.; Barden, R.; Preusel, J. Optical sensor for determining the degree of polymerization of the insulation paper inside transformers. *Transform. Mag.* **2021**, *8*, 106–117.
172. Lee, C.L.; Chin, K.L.; H'Ng, P.S.; Hafizuddin, M.S.; Khoo, P.S. Valorisation of Underutilized Grass Fibre (Stem) as a Potential Material for Paper Production. *Polymers* **2022**, *14*, 5203. [[CrossRef](#)]
173. Azis, N.; Liu, Q.; Wang, Z.D. Ageing assessment of transformer paper insulation through post mortem analysis. *IEEE Trans. Dielectr. Electr. Insul.* **2014**, *21*, 845–853. [[CrossRef](#)]
174. Lv, Y.; Zhou, Y.; Li, C.; Ge, Y.; Qi, B. Creeping Discharge Characteristics of Nanofluid-Impregnated Pressboards Under AC Stress. *IEEE Trans. Plasma Sci.* **2016**, *44*, 2589–2593. [[CrossRef](#)]
175. Yuan, Y.; Liao, R. A Novel Nanomodified Cellulose Insulation Paper for Power Transformer. *J. Nanomater.* **2014**, *2014*, 1–6. [[CrossRef](#)]
176. Hollertz, R.; Wågberga, L.; Pitois, C. Novel cellulose nanomaterials. In Proceedings of the 2014 IEEE 18th International Conference on Dielectric Liquids (ICDL), Bled, Slovenia, 29 June–3 July 2014; pp. 1–4.
177. Xiang, M.; Liao, R.; Wang, J.; Liang, N.; Lv, Y. Investigation on the effects of KH550 on the properties of alumina nanoparticles modified paper. In Proceedings of the 2016 IEEE International Conference on High Voltage Engineering and Application (ICHVE), Chengdu, China, 19–22 September 2016.
178. Huang, J.; Zhou, Y.; Dong, L.; Zhou, Z.; Liu, R. Enhancement of mechanical and electrical performances of insulating presspaper by introduction of nanocellulose. *Compos. Sci. Technol.* **2017**, *138*, 40–48. [[CrossRef](#)]
179. Chen, Q.; Liu, H.; Chi, M.; Wang, Y.; Wei, X. Experimental Study on Influence of Trap Parameters on Dielectric Characteristics of Nano-Modified Insulation Pressboard. *Materials* **2017**, *10*, 90. [[CrossRef](#)] [[PubMed](#)]
180. Pérez-Rosa, D.; García, B.; Burgos, J.C. Influence of Nanoparticles on the Degradation Processes of Ester-Based Transformer Insulation Systems. *Energies* **2022**, *15*, 1520. [[CrossRef](#)]
181. Ibrahim, A.; Nasrat, L.; Elnoby, A.; Eldebeiky, S. Thermal ageing study of ZnO nanofluid–cellulose insulation. *IET Nanodielectrics* **2020**, *3*, 124–130. [[CrossRef](#)]
182. Pradhan, A.K.; Koley, C.; Chatterjee, B.; Chakravorti, S. Determination of optimized slope of triangular excitation for condition assessment of oil-paper insulation by frequency domain spectroscopy. *IEEE Trans. Dielectr. Electr. Insul.* **2016**, *23*, 1303–1312. [[CrossRef](#)]

183. Chakraborty, B.; Raj, K.; Pradhan, A.; Chatterjee, B.; Chakravorti, S.; Dalai, S. Investigation of Dielectric Properties of TiO<sub>2</sub> and Al<sub>2</sub>O<sub>3</sub> nanofluids by Frequency Domain Spectroscopy at Different Temperatures. *J. Mol. Liq.* **2021**, *330*, 115642. [[CrossRef](#)]
184. Sheykhnazari, S.; Tabarsa, T.; Mashkour, M.; Khazaeian, A.; Ghanbari, A. Multilayer bacterial cellulose/resole nanocomposites: Relationship between structural and electro-thermo-mechanical properties. *Int. J. Biol. Macromol.* **2018**, *120*, 2115–2122. [[CrossRef](#)] [[PubMed](#)]
185. Mo, Y.; Yang, L.; Hou, W.; Zou, T.; Huang, Y.; Zheng, X.; Liao, R. Preparation of cellulose insulating paper of low dielectric constant by OAPS grafting. *Cellulose* **2019**, *26*, 7451–7468. [[CrossRef](#)]
186. Le Bras, D.; Strømme, M.; Mihranyan, A. Characterization of Dielectric Properties of Nanocellulose from Wood and Algae for Electrical Insulator Applications. *J. Phys. Chem. B* **2015**, *119*, 5911–5917. [[CrossRef](#)]
187. Tang, C.; Chen, R.; Zhang, J.; Peng, X.; Chen, B.; Zhang, L. A review on the research progress and future development of nano-modified cellulose insulation paper. *Iet Nanodielectrics* **2022**, *5*, 63–84. [[CrossRef](#)]
188. Yan, S.; Liao, R.; Yang, L.; Zhao, X.; Yuan, Y.; He, L. Influence of nano-Al<sub>2</sub>O<sub>3</sub> on electrical properties of insulation paper under thermal aging. In Proceedings of the 2016 IEEE International Conference on High Voltage Engineering and Application (ICHVE), Chengdu, China, 19–22 September 2016.
189. Oparanti, S.O.; Khaleed, A.A.; Abdelmalik, A.A.; Chalashkanov, N.M. Dielectric characterization of palm kernel oil ester-based insulating nanofluid. In Proceedings of the 2020 IEEE Conference on Electrical Insulation and Dielectric Phenomena (CEIDP), East Rutherford, NJ, USA, 18–30 October 2020; pp. 211–214.
190. Cimbala, R.; Bucko, S.; Kruželák, L.; Kostelec, M. Thermal degradation of transformer pressboard impregnated with magnetic nanofluid based on transformer oil. In Proceedings of the 2017 18th International Scientific Conference on Electric Power Engineering (EPE), Kouty nad Desnou, Czech Republic, 17–19 May 2017; pp. 1–5.
191. Lv, Y.; Ge, Y.; Li, C.; Wang, Q.; Zhou, Y.; Qi, B.; Yi, K.; Chen, X.; Yuan, J. Effect of TiO<sub>2</sub> nanoparticles on streamer propagation in transformer oil under lightning impulse voltage. *IEEE Trans. Dielectr. Electr. Insul.* **2016**, *23*, 2110–2115. [[CrossRef](#)]
192. Oparanti, S.O.; Khaleed, A.A.; Abdelmalik, A.A. Nanofluid from palm kernel oil for high voltage insulation. *Mater. Chem. Phys.* **2021**, *259*, 123961. [[CrossRef](#)]
193. Oparanti, S.O.; Adekunle, A.A.; Oteikwu, V.E.; Galadima, A.I.; Abdelmalik, A.A. An experimental investigation on composite methyl ester as a solution to environmental threat caused by mineral oil in transformer insulation. *Biomass-Converts. Biorefinery* **2022**, 1–11. [[CrossRef](#)]
194. Revathi, B.; Rajamani, M. Investigations on the flashover characteristics of ester oil impregnated pressboard under the influence of na-noparticles. In Proceedings of the 2015 IEEE International Conference on Electrical, Computer and Communication Technologies (ICECCT), Coimbatore, India, 5–7 March 2015; pp. 1–5.
195. El-Refai, E.-S.M.; Elrahman, M.K.A.; Abdo, M.H.; Mansour, D.-E.A. Electrical discharge analysis on nanofluid/pressboard surface under AC voltage application. In Proceedings of the 2017 Nine-teenth International Middle East Power Systems Conference (MEPCON), Cairo, Egypt, 19–21 December 2017; pp. 1048–1052.
196. Huang, M.; Ying, Y.; Liu, B.; Lv, Y.; Qi, B.; Li, C. Enhanced voltage distribution and breakdown strength performances of oil-paper composite insulation by adding TiO<sub>2</sub> nanoparticles. *High Volt.* **2021**, *6*, 42–50. [[CrossRef](#)]
197. Liu, D.; Deng, C.G.; Xu, X.; Jing, Y.; Li, X.; Noubissi, R.K.; Li, X. Investigation on heating aging mechanism of cellulose paper for oil-immersed transformer main insulation. In Proceedings of the 2019 IEEE 20th International Conference on Dielectric Liquids (ICDL), Roma, Italy, 23–27 June 2019; pp. 1–3.
198. Shan, B.; Ying, Y.; Huang, M.; Niu, M.; Qi, B.; Li, C.; Sun, Q.; Lv, Y. Effect of TiO<sub>2</sub> nanoparticles on DC breakdown performance of transformer oil-impregnated pressboard. *IEEE Trans. Dielectr. Electr. Insul.* **2019**, *26*, 1998–2004. [[CrossRef](#)]
199. Abd-Elhady, A.M.; Abdul-Aleem, A.A.; Izzularab, M.A. Electrical properties evaluation of double-layer nano-filled oil-paper composites. *IET Sci. Meas. Technol.* **2021**, *15*, 77–84. [[CrossRef](#)]
200. Du, B.; Liu, Q.; Shi, Y.; Zhao, Y. The Effect of Fe<sub>3</sub>O<sub>4</sub> Nanoparticle Size on Electrical Properties of Nanofluid Impregnated Paper and Trapping Analysis. *Molecules* **2020**, *25*, 3566. [[CrossRef](#)] [[PubMed](#)]
201. Pérez-Rosa, D.; Montero, A.; García, B.; Burgos, J.C. Dielectric Strength of Nanofluid-Impregnated Transformer Solid Insulation. *Nanomaterials* **2022**, *12*, 4128. [[CrossRef](#)]
202. Qi, B.; Wei, Z.; Li, C. Creepage discharge of oil-pressboard Insulation in AC-DC composite field: Phenomenon and characteristics. *IEEE Trans. Dielectr. Electr. Insul.* **2016**, *23*, 237–245. [[CrossRef](#)]
203. Thirumurugan, C.; Kumbhar, G.B.; Oruganti, R. Surface Discharge Characteristics of Different Solid-Liquid Insulation Materials in Power Transformers. *IEEE Trans. Plasma Sci.* **2019**, *47*, 5013–5022. [[CrossRef](#)]
204. Liu, Q.; Wang, Z.D. Streamer characteristic and breakdown in synthetic and natural ester transformer liquids under standard lightning impulse voltage. *IEEE Trans. Dielectr. Electr. Insul.* **2011**, *18*, 285–294. [[CrossRef](#)]
205. Wilson, M.P.; Timoshkin, I.V.; Given, M.J.; Macgregor, S.J.; Sinclair, M.A.; Thomas, K.J.; Lehr, J.M. Effect of applied field and rate of voltage rise on surface breakdown of oil-immersed polymers. *IEEE Trans. Dielectr. Electr. Insul.* **2011**, *18*, 1003–1010. [[CrossRef](#)]
206. Li, C.; Lin, C.; Zhang, B.; Li, Q.; Liu, W.; Hu, J.; He, J. Understanding surface charge accumulation and surface flashover on spacers in compressed gas insulation. *IEEE Trans. Dielectr. Electr. Insul.* **2018**, *25*, 1152–1166. [[CrossRef](#)]
207. Dai, J.; Wang, Z.D.; Jarman, P. Creepage discharge on insulation barriers in aged power transformers. *IEEE Trans. Dielectr. Electr. Insul.* **2010**, *17*, 1327–1335. [[CrossRef](#)]

208. Michelarakis, M.; Widger, P.; Beroual, A.; Haddad, A. Electrical Detection of Creeping Discharges over Insulator Surfaces in Atmospheric Gases under AC Voltage Application. *Energies* **2019**, *12*, 2970. [[CrossRef](#)]
209. Sun, G.-Y.; Guo, B.-H.; Song, B.-P.; Su, G.-Q.; Mu, H.-B.; Zhang, G.-J. Simulation on the dynamic charge behavior of vacuum flashover developing across insulator involving outgassing. *Phys. Plasmas* **2018**, *25*, 063502. [[CrossRef](#)]
210. Zhao, Z.; Huang, D.D.; Wang, Y.N.; He, J.X.; Li, C.J.; Wang, Y.F.; Li, J.T. Evolution of streamer dynamics and discharge mode transition in high-pressure nitrogen under long-term repetitive nanosecond pulses with different time-scales. *Plasma Sources Sci. Technol.* **2019**, *28*, 085015. [[CrossRef](#)]
211. Madhar, S.A.; Mráz, P.; Mor, A.R.; Ross, R. Study of corona configurations under DC conditions and recommendations for an identification test plan. *Int. J. Electr. Power Energy Syst.* **2020**, *118*, 105820. [[CrossRef](#)]
212. Zhao, J.; An, Z.; Lv, B.; Wu, Z.; Zhang, Q. Characteristics of the Partial Discharge in the Development of Conductive Particle-Initiated Flashover of a GIS Insulator. *Energies* **2020**, *13*, 2481. [[CrossRef](#)]
213. Zhou, Y.; Jin, F.; Huang, M.; Sha, Y.; Zhang, L.; Huang, J. Influence of temperature on developing process of surface flashover in oil-paper insulation under combined AC-DC voltage. In Proceedings of the 2013 Annual Report Conference on Electrical Insulation and Dielectric Phenomena, Shenzhen, China, 20–23 October 2013; pp. 486–489.
214. Rafiq, M.; Chengrong, L.; Lv, Y. Effect of Al<sub>2</sub>O<sub>3</sub> nanorods on dielectric strength of aged transformer oil/paper insulation system. *J. Mol. Liq.* **2019**, *284*, 700–708. [[CrossRef](#)]
215. Lv, Y.Z.; Zhou, Y.; Li, C.R.; Ma, K.B.; Wang, Q.; Wang, W.; Zhang, S.N.; Jin, Z.Y. Nanoparticle effects on creeping flashover characteristics of oil/pressboard interface. *IEEE Trans. Dielectr. Electr. Insul.* **2014**, *21*, 556–562. [[CrossRef](#)]
216. Abdul-Aleem, A.A.; Abd-Elhady, A.M.; Izzularab, M.A. Experimental evaluation of creeping flashover at nanofilled oil/pressboard interface. In Proceedings of the 2017 Nineteenth International Middle East Power Systems Conference (MEPCON), Cairo, Egypt, 19–21 December 2017; pp. 695–701.
217. Ge, Y.; Lv, Y.; Han, Q.; Sun, Q.; Huang, M.; Li, C.; Qi, B.; Yuan, J. Effects of TiO<sub>2</sub> Nanoparticles on Streamer Propagation at the Surface of Oil-Impregnated Insulation Paper. *IEEE Trans. Plasma Sci.* **2018**, *46*, 2491–2496. [[CrossRef](#)]
218. Huang, M.; Han, Q.-B.; Lv, Y.-Z.; Wang, L.; Shan, B.-L.; Ge, Y.; Qi, B.; Li, C.-R. Effect of nanoparticle shapes on creeping flashover characteristics at the interface of nanofluid-impregnated pressboard. *IEEE Trans. Dielectr. Electr. Insul.* **2018**, *25*, 1135–1141. [[CrossRef](#)]
219. Shan, B.; Huang, M.; Ying, Y.; Niu, M.; Sun, Q.; Lv, Y.; Li, C.; Qi, B.; Xing, Z. Research on creeping flashover characteristics of nanofluid-impregnated pressboard modified based on Fe<sub>3</sub>O<sub>4</sub> nanoparticles under lightning impulse voltages. *Nanomaterials* **2019**, *9*, 524. [[CrossRef](#)]
220. El-Refai, E.-S.M.; Mansour, D.-E.A.; Elrahmen, M.A.; Abdo, M.H. Enhancing flashover strength along oil/pressboard interface using nanofluids. *Alex. Eng. J.* **2020**, *59*, 475–483. [[CrossRef](#)]
221. Abu-Elanien, A.E.; Salama, M. Asset management techniques for transformers. *Electr. Power Syst. Res.* **2010**, *80*, 456–464. [[CrossRef](#)]
222. Zhou, H.; Li, X.; Zhu, Y.; Liu, J.; Wu, A.; Ma, G.; Wang, X.; Jia, Z.; Wang, L. Review of flash sintering with strong electric field. *High Volt.* **2021**, *7*, 1–11. [[CrossRef](#)]
223. Ilkhechi, H.D.; Samimi, M.H.; Yousefvand, R. Generation of acoustic phase-resolved partial discharge patterns by utilizing UHF signals. *Int. J. Electr. Power Energy Syst.* **2019**, *113*, 906–915. [[CrossRef](#)]
224. Pan, C.; Wu, K.; Chen, G.; Gao, Y.; Florkowski, M.; Lv, Z.; Tang, J. Understanding Partial Discharge Behavior from the Memory Effect Induced by Residual Charges: A Review. *IEEE Trans. Dielectr. Electr. Insul.* **2020**, *27*, 1951–1965. [[CrossRef](#)]
225. Cheng, Y.; Zhang, S.; Mao, T.; Guo, S.; Niu, Z.; Hao, Z. Propagation Mechanism of Carbonized Trees in Oil-cellulose Insulation Systems of Power Transformers. In Proceedings of the 2020 IEEE Electrical Insulation Conference (EIC), Knoxville, TN, USA, 22 June–July 2020; pp. 486–489.
226. Liu, D.; Wu, Y.; Xu, X.; Ye, J.; Li, J.; Yu, S.; Li, X. Suppression Mechanism of TiO<sub>2</sub> for the Partial Discharge of Oil-paper Insulation in Intensive Electric Field. In Proceedings of the 2019 IEEE 20th International Conference on Dielectric Liquids (ICDL), Roma, Italy, 23–27 June 2019; pp. 1–4.
227. Chen, G.; Fu, M.; Liu, X.Z.; Zhong, L.S. ac aging and space-charge characteristics in low-density polyethylene polymeric insulation. *J. Appl. Phys.* **2005**, *97*, 083713. [[CrossRef](#)]
228. Huang, M.; Zhou, Y.; Chen, W.; Sha, Y.; Jin, F. Influence of voltage reversal on space charge behavior in oil-paper insulation. *IEEE Trans. Dielectr. Electr. Insul.* **2014**, *21*, 331–339. [[CrossRef](#)]
229. Wang, F.; He, L.; Khan, M.Z.; Zhang, T.; Zhao, Q.; He, Y.; Huang, Z.; Zhao, H.; Li, J. Accelerated Charge Dissipation by Gas-Phase Fluorination on Nomex Paper. *Appl. Sci.* **2019**, *9*, 3879. [[CrossRef](#)]
230. Mo, Y.; Yuan, Y.; Liao, R. Study on improving the space charge behavior in insulating paper by depositing nanostructured alumina on its surface via magnetron sputtering. *Thin Solid Film.* **2020**, *709*, 138219. [[CrossRef](#)]
231. Wu, K.; Zhu, Q.; Wang, H.; Wang, X.; Li, S. Space charge behavior in the sample with two layers of oil-immersed-paper and oil. *IEEE Trans. Dielectr. Electr. Insul.* **2014**, *21*, 1857–1865. [[CrossRef](#)]
232. Min, X.; Yuan, Y.; Ruijin, L. Improvement in space charge behavior of cellulose paper by coating with AlO<sub>x</sub> nanostructure film. *Mater. Lett.* **2018**, *230*, 253–256. [[CrossRef](#)]
233. Li, L.; Zhao, Z. Effect of switch parameters and polarity on the repetitive performance of a corona-stabilized switch viewed from behavior of space charge. *Phys. Plasmas* **2020**, *27*, 043509. [[CrossRef](#)]

234. Li, J.; Wang, Y.; Bao, L. Space Charge Behavior of Oil-Impregnated Paper Insulation Aging at AC-DC Combined Voltages. *J. Electr. Eng. Technol.* **2014**, *9*, 635–642. [[CrossRef](#)]
235. Wang, Y.; Wu, J.; Yin, Y. Space Charge and Trap in High-Voltage Power Module Packaging Insulation: Simultaneous Measurement and 2-D Simulation. *IEEE Trans. Dielectr. Electr. Insul.* **2022**, *29*, 1400–1408. [[CrossRef](#)]
236. Hao, M.; Zhou, Y.; Chen, G.; Wilson, G.; Jarman, P. Space charge behavior in thick oil-impregnated pressboard under HVDC stresses. *IEEE Trans. Dielectr. Electr. Insul.* **2015**, *22*, 72–80. [[CrossRef](#)]
237. Huang, M.; Zhou, Y.; Chen, W.; Lu, L.; Jin, F.; Huang, J. Space charge dynamics at the physical interface in oil-paper insulation under DC voltage. *IEEE Trans. Dielectr. Electr. Insul.* **2015**, *22*, 1739–1746. [[CrossRef](#)]
238. Wei, Y.; Han, W.; Li, G.; Liang, X.; Gu, Z.; Hu, K. Aging Characteristics of Transformer Oil-Impregnated Insulation Paper Based on Trap Parameters. *Polymers* **2021**, *13*, 1364. [[CrossRef](#)]
239. Sun, P.; Sima, W.; Zhang, D.; Jiang, X.; Zhang, H.; Yin, Z. Failure Characteristics and Mechanism of Nano-Modified Oil-Impregnated Paper Subjected to Repeated Impulse Voltage. *Nanomaterials* **2018**, *8*, 504. [[CrossRef](#)]
240. Liao, R.J.; Lv, C.; Yang, L.J.; Zhang, Y.Y.; Liu, T. Space charge behavior in oil-impregnated insulation paper reinforced with nano-TiO<sub>2</sub>. *BioResources* **2013**, *8*, 5655–5665. [[CrossRef](#)]
241. Liao, R.; Wang, J.; Gao, F.; Yuan, Y.; Xu, Z. Effects of aluminum nitride nanoparticles on the space charge behavior of cellulose paper. *J. Mater. Sci.* **2016**, *51*, 10701–10713. [[CrossRef](#)]

**Disclaimer/Publisher’s Note:** The statements, opinions and data contained in all publications are solely those of the individual author(s) and contributor(s) and not of MDPI and/or the editor(s). MDPI and/or the editor(s) disclaim responsibility for any injury to people or property resulting from any ideas, methods, instructions or products referred to in the content.